Available online at www.sciencedirect.com
SCIENCE DIRECT®
Applied Geochemistry 21 (2006) 58–82
Applied Geochemistry
www.elsevier.com/locate/apgeochem

Atmospheric Pb-pollution by pre-medieval mining detected in the sediments of the brackish karst lake An Loch Mór, western Ireland

G. Schettler *, R.L. Romer

GeoForschungsZentrum Potsdam, Telegrafenberg, D-14473 Potsdam, Germany

Received 22 September 2004; accepted 20 September 2005
Editorial handling by R. Fuge
Available online 23 November 2005

Abstract

This paper presents results of geochemical investigations of lake sediments from the karst lake An Loch Mór, Aran Islands, including the first highly resolved record of atmospheric Roman Pb pollution for Ireland. The natural Pb influx into the lake is largely contributed by 3 Pb components, which differ in their isotopic composition: detrital influx of Pb from the siliciclastic input, dissolved influx of Pb released by weathering of the local limestone, and dissolved influx of seawater Pb. The balance between the 3 Pb components varies in concert with the hydrological evolution of the lake. The influx of Pb in dissolved form is estimated by geochemical mass balance assuming that the siliciclastic influx is characterised by the Pb/Al-ratio of the Late Glacial clastic sediments. It typically accounts for 50–80% of total Pb input in the Holocene sediments of An Loch Mór. The natural dissolved influxes of Pb, Sc, and Y reach a similar order of magnitude. Normalisation with Sc and Y is applied to quantify contributions from anthropogenic Pb. Based on continuous sampling of 1 cm sample slices, variations in the influx of Roman Pb could be reconstructed at a time resolution of c. 5 a. Combined geochemical and Pb isotope mass balance is used to characterise the isotopic composition of anthropogenic Pb. Distinctly enhanced influx of anthropogenic Pb occurs in the 1st and 2nd century AD and shows high variability on decadal scale. This is in contrast to central European Pb records, which document a gradual increase and decrease in ancient atmospheric pollution by Roman Pb. The reconstructed high variability in the influx of Roman Pb in An Loch Mór documents variations in the wind regime of western Europe, temporarily favouring the transport of atmospheric Pb to western Ireland.

1. Introduction

In industrial areas, the release of anthropogenic Pb into the atmosphere by mining and metallurgical processes, burning of fossil fuels, and extensive use of leaded gasoline from the 1950s to the 1970s in North America and until the 1980s in Europe (Candelone and Hong, 1995) reached such a magnitude that it became readily detectable by increasing total Pb contents in various kinds of natural monitors (see Nriagu and Pacyna (1988) for estimates of contributions from different sources). A high-resolution sediment record from Lake Erie, for instance, indicates a maximum in airborne Pb pollution for the north-eastern

* Corresponding author. Fax: +49 3312881302.
E-mail address: schet@gfz-potsdam.de (G. Schettler).

0883-2927/$ - see front matter
doi:10.1016/j.apgeochem.2005.09.009

Unites States in 1972 (Graney et al., 1995). The record of modern Pb pollution from a blanket bog in western Ireland (Bellacorick Bog, 56°6′ N, 9°34′ W; Schell et al., 1997) documents that atmospheric deposition of Pb reached a maximum of 4 mg m^{-2} a^{-1} around 1970. Similarly, atmospheric Pb deposition at Summit (central Greenland) was at its maximum around 1970 (Candelone and Hong, 1995).

Aeolian influx of anthropogenic Pb originating from metallurgical processing of Pb ores in the pre-industrial period has also been detected in a growing number of palaeoenvironmental archives during the last decade (Fig. 1). Most of these records are not located close to ancient mining sites and, therefore, document large-scale atmospheric pollution. The broad geographic distribution of archives with ancient Pb contamination raises the question of synchroneity in the onset, peak, and decline of anthropogenic Pb-influx and its variability (Renberg et al., 2001).

Pre-industrial atmospheric deposition of Pb released at ancient mining and smelting sites can be detected in various natural monitors, for instance, in Greenland ice core records (Hong et al., 1994; Rosman et al., 1997), in British (Lee and Tallis, 1973; Livett et al., 1979; West et al., 1997), Scandinavian (Brännvall et al., 1997), central European (Shotyk et al., 1998; Kempter et al., 1997), and Iberian bogs (Martínez-Cortizas et al., 1997), as well as in European lacustrine sediment profiles (Renberg et al., 1994; Brännvall et al., 1997; Schettler and Romer, 1998; Garbe-Schönberg et al., 1998; Renberg et al., 2001; Brännvall et al., 2001). In general, ombrotrophic bogs, and snow and ice records, which document aeolian Pb-influx only, represent more sensitive archives for ancient atmospheric Pb pollution than lacustrine sediments that receive additional input of Pb by groundwater inflow and surface run-off. The distribution of Pb released into the atmosphere at ancient mining and smelting sites (anthropogenic Pb) is closely related to the wind regime, which may vary on diurnal, seasonal, and decadal time scales. Atmospheric Pb is removed from the atmosphere by dry and wet deposition. Since wet deposition of aerosols proceeds more efficiently than dry deposition of micro-sized particles, deposition of atmospheric Pb might be positively correlated with precipitation frequency. The atmospheric Pb concentration of air masses loaded with anthropogenic Pb emissions, however, depends on their out-wash history. The atmospheric deposition of anthropogenic Pb emissions commonly declines with increasing distance from the source area (e.g. Telmer et al., 2004). Long-range transport of Pb is favoured for conditions that support the ascent of Pb into high tropospheric levels.

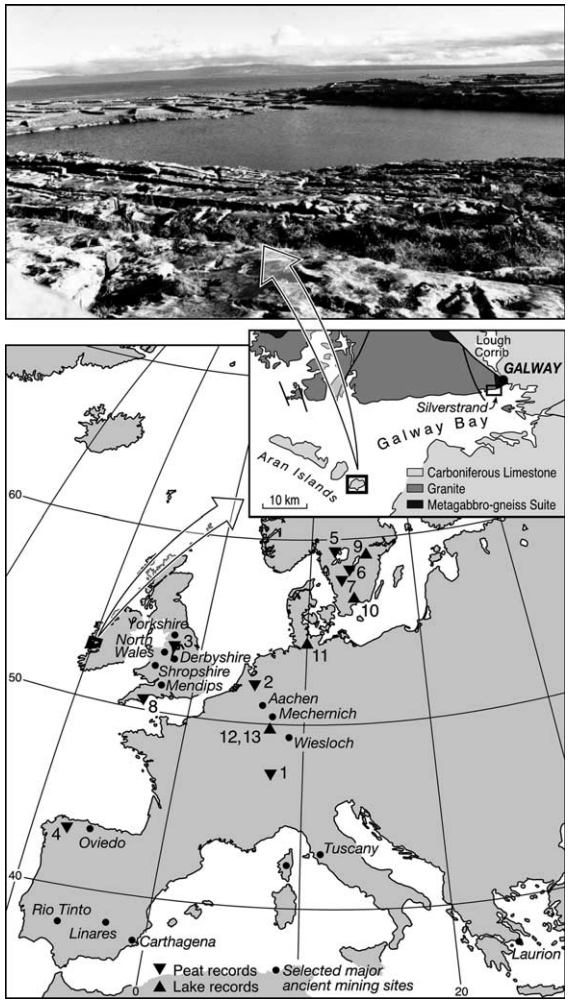

Fig. 1. Above: The setting of Lake Loch An Mór in the karst landscape of Inis Oírr. Below: Map of Europe showing major Roman mining sites and selected locations with sediment records that document aeolian influx of Roman Pb, 1 Etang de la Gruere, Jura mountains (CH), 2 Engbertsdijksveen (NL), 3 Featherbed Moss (Derbyshire, GB), 4 Penido Vello bog (SP), 5 Önneby Mosse, 6 Trolls Mosse, 7 Store Moss (all S), 8 TOR Royal (Devon GB), 9 Gardsjön (S), 10 Rudegyl (S), 11 Belau (Schleswig-Holstein, GER), 12 Meerfelder Maar, and Schalkenmehrener Maar (W. Eifel, GER). Inset shows location of Aran Islands on the western coast of Ireland.

For the detection and quantification of minor atmospheric Pb pollution in the pre-industrial period, variations in the geogenic influx of Pb have to be considered. In many natural monitors, the influx of the trace element Pb is positively correlated with influx of siliciclastic matter by aeolian and fluvial

input. Influx of soil particles by surface run-off and natural aeolian deposition (e.g. mineral and seawater aerosols) varies with climate change and human impact. Influx of anthropogenic Pb becomes detectable by normalisation using conservative major or minor elements. Divalent Pb released by silicate weathering is immobilised by surface sorption and gets enriched in the clay-size fraction or by scavenging on Fe-oxyhydroxides. Variations in bulk geochemical characteristics and in grain-size composition of the siliciclastic input, therefore, have to be considered for the assessment of anthropogenic Pb input. Contributions from anthropogenic Pb may also become apparent in the Pb-isotope record of natural monitors, if the bulk geogenic influx of Pb and the anthropogenic Pb component differ in their isotopic composition. The geogenic influx of Pb, however, can also vary in its isotopic composition, for instance, by changes in the balance between local and remote siliciclastic components of the bulk allochthonous input (e.g. Schettler and Romer, 1998).

Atmospheric Pb pollution on a hemispherical scale since the middle of the first millennium BC has been detected in Greenland ice-records (Hong et al., 1994; Rosman et al., 1997). For the pre-Medieval period, European lake and bog records document a 2–3 orders of magnitude higher aeolian influx of anthropogenic Pb than for Greenland, with a maximum in the Roman period. Dating and quantification of Roman Pb records from various European sites offers the possibility of reconstructing spatial and temporal variations in atmospheric Pb pollution by mining and metallurgical processing of Pb ores during the Roman period. In this study, the authors investigate pre-Medieval atmospheric deposition of anthropogenic Pb for western Ireland based on a detailed study of a continuous Holocene sediment record from the brackish karst lake An Loch Mór. To authors' knowledge, no previous work of this nature has been carried out in western Ireland. Westerly wind directions favour the atmospheric transport of Pb emissions from the major Roman mining sites of Pb ores to central Europe (Fig. 1), whereas the atmospheric transport of Roman Pb to Ireland requires southerly or easterly winds that occur only occasionally.

2. Site description, characterisation of the sediment record and chronology

An Loch Mór lies in a closed, deep basin on Inis Oírr, the smallest (586 ha) of the Aran Islands (Irish National Grid ref. L 990 020; 9°30.3′W, 53°03.5′N; Fig. 1). It measures approximately 620 × 220 m, has an area of 9.2 ha and a maximum water depth of 23 m. It lies at sea level and is separated from the Atlantic Ocean by only c. 250 m of low-lying, jointed limestone at its northern end (Fig. 1). The bedrock consists of karstified Lower Carboniferous limestone. Though glaciated during the last and previous glaciations, obvious glacial deposits are confined to occasional granite erratics transported from the north. Soils, where present, are of plaggen origin, i.e., they consist mainly of sand and seaweed taken from the shore and brought into small fields enclosed by high stone walls that provide shelter and reduce soil erosion by wind.

The chronology of the An Loch Mór sedimentation record relies on several lines of evidence including AMS ^{14}C dates (mainly terrestrial plant remnants, van der Plicht, in TIMECHS, 2001), tephrochronomarkers (Chambers et al., 2004), pollen stratigraphy (Molloy and O'Connell, 2004), as well as varve analysis (Saarinen, in TIMECHS, 2001) and ^{210}Pb and ^{137}Cs profiles (Heijnis, in TIMECHS, 2001). Fig. 2 shows an age/depth plot that represents the 'best approximation' based on a synthesis of all the relevant data (details will be published elsewhere). AMS ^{14}C dates of the upper sediment section are derived mainly from pieces of aquatic mosses and appear to be influenced by a hard-water effect.

Sedimentation in An Loch Mór was strongly influenced by the hydrological evolution of the lake. The relation between biogenic production and carbonate deposition is sensitive to the balance between seawater and freshwater influx and the overall magnitude of these fluxes (Schettler et al., submitted). The freshwater inflow depends on precipitation and evapotranspiration (EVPT), which is high for closed woody vegetation. Thus, freshwater inflow depends on climate and vegetation dynamics. Seawater input varied with the post-glacial rise of the sea level from sea spray deposition through occasional infiltration to diurnal ingression from c. 5100 cal. BP. Diurnal seawater infiltration is controlled by the freshwater discharge from the catchment and is less important at times of high freshwater inflow. The net accumulation of autochthonous calcite and organic matter largely determines Holocene sedimentation in An Loch Mór, siliciclastic input is only minor (Schettler et al., submitted). Precipitation of autochthonous calcite increases with enhanced groundwater inflow from the catchment. Influx of nutrient-rich seawater

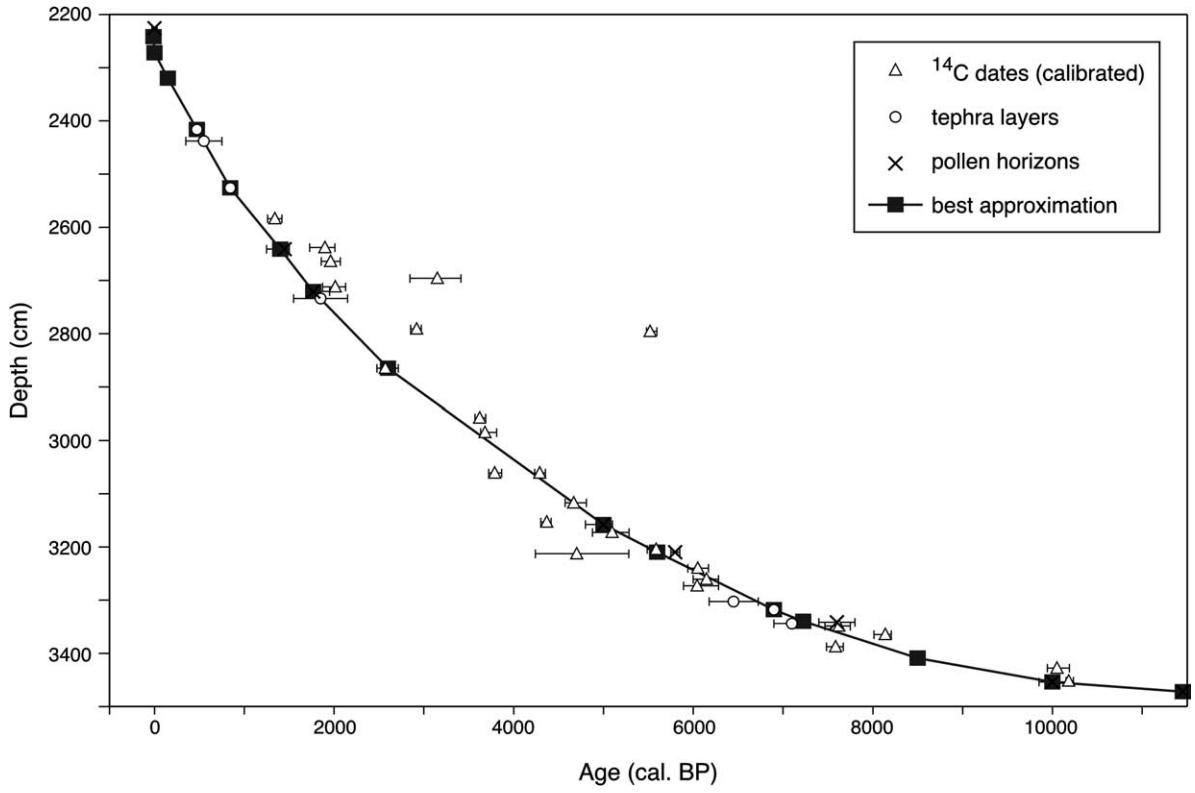

Fig. 2. Age/depth relationship for the composite profile of An Loch Mór sediments, calibration of AMS ^{14}C dates based on the CALIB 4.3 program of Stuiver and Reimer with data from Stuiver et al. (1998).

forces photosynthetic production in the lake and inhibits the precipitation of calcite. Variations in the freshwater to seawater balance are geochemically recorded in the An Loch Mór sediments by systematic variations of the total organic C (TOC), $CaCO_3$, Ca/Sr, and Ca/Mg profiles (Schettler et al., submitted). The aluminosilicate concentration of the sediments decreased during the early Holocene. Bulk trace element concentrations (including Pb) are substantially derived from the dissolved influx.

The geochemical signatures of the calcareous late Younger Dryas (YD) sediments are similar in their chemical and mineralogical signatures with the fine fractions of calcareous regional drift. The decline of Al_2O_3 during the early Holocene sedimentation (Fig. 3) may reflect the erosion of relict till on the island. Even at their lower limit, the Al_2O_3 concentration of the sediments exceeds the mean Al_2O_3 contents of modern calcareous soils (0.47 wt%) and local clastic components, such as the Carboniferous limestone bedrock (0.05 wt% Al_2O_3) and sand dune deposits (0.13 wt% Al_2O_3), that might contribute to the detrital influx (Table 1). Early Holocene sediment sections show enhanced Al/Ti ratios (~27), which are typical of the clay fraction in the till ($Till_{clay}$), whereas younger sediments are characterised by generally lower Al/Ti (~20, Fig. 3). It is unclear whether the siliciclastic fraction of the Holocene sediments is still dominated by the residue of chemically dissolved local calcareous components, mainly till (2.8 wt% Al_2O_3), or whether remote siliciclastic components became more significant in the course of the Holocene.

3. Methodology

Three sediment cores, MOR1, MOR2, and MOR3, were recovered in 2-m long drives in close proximity to each other from the deepest part of the lake basin using an Usinger piston corer (the diameter of the coring tubes was 8 cm, for individual core sites, see Molloy and O'Connell, 2004). Water depth at the coring sites was c. 22.6 m. The 2-m long core segments were extruded in the field immediately after core recovery, cut along their

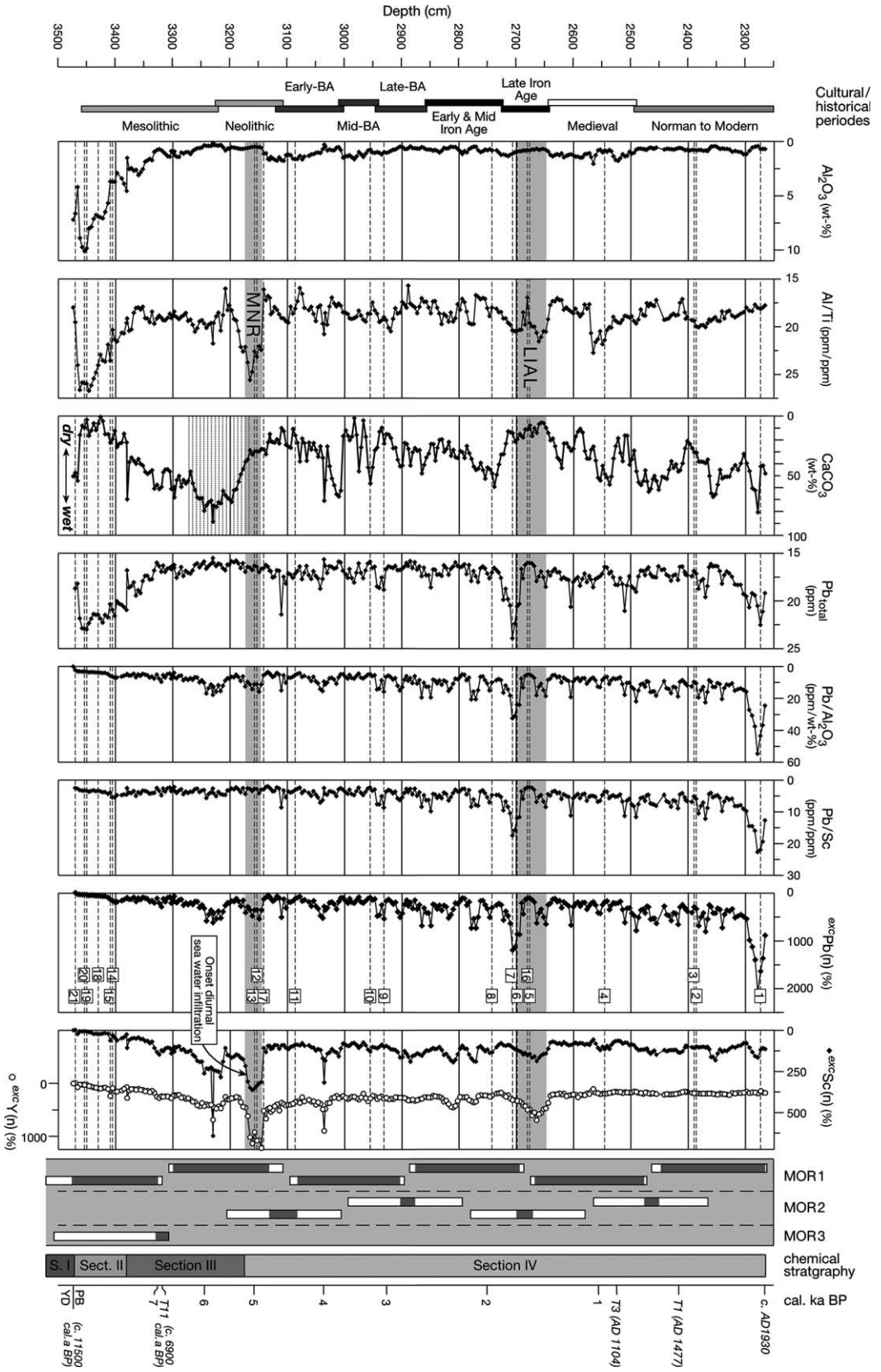
Depth (cm)
3500
3400
3300
3200
3100
3000
2900
2800
2700
2600
2500
2400
2300
Early-BA
Late-BA
Late Iron Age
Mesolithic
Neolithic
Mid-BA
Early & Mid Iron Age
Medieval
Norman to Modern
Cultural/ historical periodes
Al2O3 (wt-%)
Al/Ti (ppm/ppm)
MNR
LIAL
dry
wet
CaCO3 (wt-%)
Pbtotal (ppm)
Pb/Al2O3 (ppm/wt-%)
Pb/Sc (ppm/ppm)
excPb(n) (%)
Onset diurnal sea water infiltration
excY(n) (%)
excSc(n) (%)
MOR1
MOR2
MOR3
S. I
Sect. II
Section III
Section IV
chemical stratgraphy
PB
YD
(c. 11500 cal.a BP)
T11 (c. 6900 cal.a BP)
cal. ka BP
T3 (AD 1104)
T1 (AD 1477)
c. AD1930

length, photographed and sealed. The presence of well-defined distinctive horizons common to all 3 cores permitted reliable core correlation, which, in turn, facilitated obtaining a continuous sediment record. The uppermost unconsolidated sediments were not recovered.

Sampling for bulk chemical analysis was carried out by continuous sampling using 1-cm thick samples. Most of the samples were taken from core MOR1 with the gaps between core sections in MOR1 being bridged by taking samples from appropriate levels in cores MOR2 or MOR3 (Fig. 3). In this way, a continuous record was obtained. The outer part of the sediments was carefully removed to avoid contamination from the steel tube of the coring device. Samples were freeze-dried and then dry-sieved (200 μm). Samples were prepared for chemical analysis by re-mixing, using a mill, of 3–5 equal-weight aliquots of individual dry-sieved 1-cm samples. Sediments between 2691 and 2730 cm with contamination from Roman Pb were additionally analysed at 1-cm sample resolution. Before digestion, samples were dried at 105 °C for 2 h. Major and trace elements were analysed by ICP-AES (IRIS, Thermo Elemental) using 0.25 g samples that were digested in Teflon beakers using a HNO_3–$HClO_4$–HF mixture. Acids of Merck Suprapur quality were used throughout. Total Pb was determined by ICP-MS (ELAN 5000A, Perkin Elmer) using internal standardisation for drift correction. Details on data acquisition and typical standard errors for the ICP-MS measurements are given in Dulski (2001). Total C (TC) was analysed by IR-spectrometry after burning aliquots in an O_2 gas flow at 1350 °C, total N was determined from the same weight aliquots by heat-conductivity detection (LECO, CNS 2000). Inorganic C (IC) was determined coulometrically after the release of CO_2 by hot phosphoric acid (1:1). Total organic C (TOC) was calculated by subtracting IC from TC.

Various local detrital materials and selected mixed and 1-cm sediment samples were analysed for their Pb isotope composition by thermal ionization mass spectrometry (TIMS). Lead was separated by ion-exchange chromatography using Biorad AG1-8X in HCl and HBr media (Romer et al., 2001). Lead was loaded together with silica gel and H_3PO_4 on Re single-filaments and analysed at 1200–1260 °C. Mass-fractionation was corrected with 0.1%/a.m.u. as established through the repeated analysis of the NBS981 Pb-standard; 2 sigma reproducibility is better than 0.1% for isotope ratios involving ^{204}Pb and better than 0.05% for $^{208}Pb/^{206}Pb$. The solid densities of the individual TIMS-samples 1–14 as determined by means of a He-Pycnometer (Micromeritics) vary between 1.6 and 2.1 g cm^{-3} with a mean value of 1.8 g cm^{-3}. The mean value is considered for flux rate calculations.

4. Results

4.1. Lead of local detrital materials

Limestone. Total Pb concentrations of six limestone samples (Table 1), which represent various stratigraphic horizons of the local Carboniferous limestone, vary between 0.4 and 0.9 ppm. The mean bedrock (L_m) has 0.66 ppm Pb and 0.05 wt% Al_2O_3. Leaching with 0.5 M HCl (samples R0, R1, R2, R3, R4, R12) demonstrates that 42–70% of total Pb in the bedrock is surface or carbonate-bound (Table 1). Sample R0, which may adequately represent the Carboniferous limestone (Schettler et al., submitted), has distinctly enhanced $^{206}Pb/^{204}Pb$ and $^{207}Pb/^{204}Pb$ ratios that originate from *in situ* growth of Pb since the deposition of the limestone (Table 2). As the limestone has very low Th contents (0.09 ppm) and, thus, low $^{232}Th/^{204}Pb$ values, there was little *in situ* growth of ^{208}Pb. Lead released by leaching of the bedrock sample R0 is uranogenic (Table 2, Fig. 4).

Fig. 3. Selected geochemical profiles recording 11.6 ka sedimentation in An Loch Mór. $^{exc}Pb(n)$ and $^{exc}Sc(n)$: calculated Pb excess, Sc excess, and Y excess normalised per 1 wt% Al_2O_3 in % relative to the bulk chemical composition of the clastic YD sediments (Y/Al_2O_3 = 2.9, Pb/Al_2O_3 = 2.5, Sc/Al_2O_3 = 0.91). The depth values are given in cm below water surface. Cultural periods for Ireland given right of the depth-axis. LIAL (Late Iron Age Lull) represents a major decline in settlement in western Ireland (e.g. O'Connell, 1994; O'Connell et al., 1987) which is also documented for Inis Oírr by regeneration of local vegetation (Molloy and O'Connell, 2004), Mid-Neolithic Regeneration (MNR) of woody vegetation on the island (Molloy and O'Connell, 2004). Hatched area in the $CaCO_3$ diagram marks the varved sediment section. Chronostratigraphic markers: Tephra layers T1, T3, and T11 correspond to T1 = Veidivötn (AD 1477), T3 = Hekla 1 (AD 1104), T11 = Lairg A (6947–6852 cal. years BP) (Chambers et al., 2004), YD-PB = Younger Dryas to Preboreal transition as indicated by palynological data. Chemical stratification documents the hydrological evolution of the Lake. Section 1: Low influx of groundwater and low limestone weathering during the YD. Section II: Seawater influx by sea spray only, Section III: Occasional intrusion of seawater, Section IV: Diurnal seawater infiltration (Schettler et al., submitted). Numbers of selected samples for Pb isotope measurements by TIMS given above the $^{exc}Pb(n)$ profile.

Table 1
Chemical characterisation of local detrital Pb-sources

Sample	$CaCO_3$[a] (wt%)	Al_2O_3 (wt%)	Al/Ti (wt%/wt%)	Pb_{total} (ppm)	Pb/Al_2O_3 (ppm/wt%)	Pb_{leach}[b] (ppm)	Pb_{leach}[b] (% of Pb_{total})	Pb_{silic}[c] (% of Pb_{total})
Bedrock (L_m)[d]		0.050	20.5	0.66	13.2		60	
Muddy Lmst.[e]		0.082	19.3	1.5	17.8			
Shale-R5		17.7	15.7	29.6	1.7	3.5	12	
$Till_{clay}$	81.4	3.8	26.9	19.5	5.1	13	67	97
$Till_{silt}$	76.1	1.81	10.7	6.6	3.6			92
T_m[f]	78.8	2.80	18.8	13.0	4.7			
YD (MOR1 VIb-75)[g]	45.0	7.34	17.7	17.3	2.4			98
YD (MOR1 VIb-76)[h]	48.9	6.77	17.6	17.6	2.6			98
Dune	76.1	0.13	22.2	1.3	10.5			
Soil[i]	91.1	0.47	16.8	3.5	7.5			79
Bedr-R0	100.1	0.06	28.9	0.47	7.6	0.31	66	
Bedr-R1	100.3	0.03	19.7	0.80	25.6	0.50	63	
Bedr-R2	101.3	0.05	22.0	0.84	15.6	0.44	53	
Bedr-R3	100.2	0.02	23.6	0.35	16.4	0.18	51	
Bedr-R4	100.2	0.07	16.6	0.89	13.0	0.62	70	
Bedr-R12	99.2	0.04	20.0	0.46	12.7	0.19	42	
S1	92.9	0.32	16.1	2.8	8.8			78
S2	95.3	0.16	18.9	1.8	11.3			65
S3	84.1	0.81	16.6	5.8	7.2			90
S5	92.0	0.58	17.1	3.6	6.3			83

[a] Based on inorganic carbon (IC).
[b] Leached with 0.5 N HCl, measured by ICP-MS.
[c] Siliciclastic-bound Pb calculated by mass-balance by subtraction of carbonate-Pb (L_m).
[d] Mean of bedrock samples R0, R1, R4, and R12. Mean does not include the individual samples R2 and R3. Sample R3 represents a bedrock section with secondary freshwater carbonate. Slightly enhanced Pb contents occur in samples R2 and R4 and were most likely introduced by interaction with Mg-rich metamorphic fluids (R2) or reflect a higher content of aluminosilicates (R4), respectively.
[e] The enhanced Pb concentration of muddy limestone in comparison with L_m could reflect both diagenetic and metamorphic enrichment (0.56 wt% MgO) as well as a higher portion of silicate-bound Pb (0.082 wt% Al_2O_3).
[f] T_m = 1:1 mixture of T_{clay} and T_{silt}.
[g] IMS sample 25.
[h] TIMS sample 26.
[i] Mean of soil samples S1, S2, S3, S5.

Table 2
Pb isotopic composition of local Pb sources

Sample	$\frac{^{206}Pb}{^{204}Pb}$	$\frac{^{207}Pb}{^{204}Pb}$	$\frac{^{208}Pb}{^{204}Pb}$	$\frac{^{208}Pb}{^{204}Pb}$
Bedrock, soil, and till samples				
Dune	22.865	15.839	38.152	1.6686
Limestone R0	31.534	16.338	38.446	1.2192
Soil (MOR 55)	23.908	15.912	38.385	1.6055
Muddy Lmst. (Till 0.5–1 mm)	20.756	15.684	38.084	1.8348
$Till_{silt}$	19.157	15.604	38.304	1.9995
$Till_{clay}$	19.058	15.598	38.399	2.0148
Leach experiments (Limestone R0)				
A 2N HCl leach	33.255	16.393	38.385	1.1543
A 2N HCl residue	28.033	16.168	38.403	1.3699
B acetic acid leach	25.931	16.072	38.382	1.4802
B 2N HCl leach	30.609	16.259	38.316	1.2518
B 2N HCl residue	37.800	16.646	38.558	1.0201
End-members for mass-balance calculations[a]				
Pb-m.E.	18.10	15.63	38.00	2.0994
Pb-$Till_{depl}$	20.10	15.73	38.60	1.9204
Pb-L_m	31.53	16.34	38.45	1.2195

[a] Pb-$Till_{depl}$, Pb-m.E., and Pb-L_m as defined in Appendix.

Shale R5. This sample represents a thin shale bed intercalated in the banked Carboniferous limestone. Shale R5 contains 0.017 wt% IC and 29.6 ppm Pb. Although its Pb/Al_2O_3 (ppm/wt%) ratio of 1.7 is higher than the corresponding value for mean continental crust composition (MCC = 1.2, Taylor, 1964), it is distinctly lower than in local calcareous materials (L_m: 13.2, T_m: 4.7, Soils: 7.5, Dune: 10.5, see Table 1 for explanation of used abbreviations), which show a significant enrichment of Pb versus Al (Table 1).

Sand dune. Local sand dunes are mainly composed of calcareous marine bioclasts and bedrock lithoclasts. The Pb isotopic composition of the dune deposit (Table 2), therefore, should represent a mixture of bedrock-Pb and seawater-Pb. The Al_2O_3 concentration (0.13 wt%) only slightly exceeds that of the bedrock mean L_m. The total Pb content of the analysed dune sample is 1.3 ppm (Table 1).

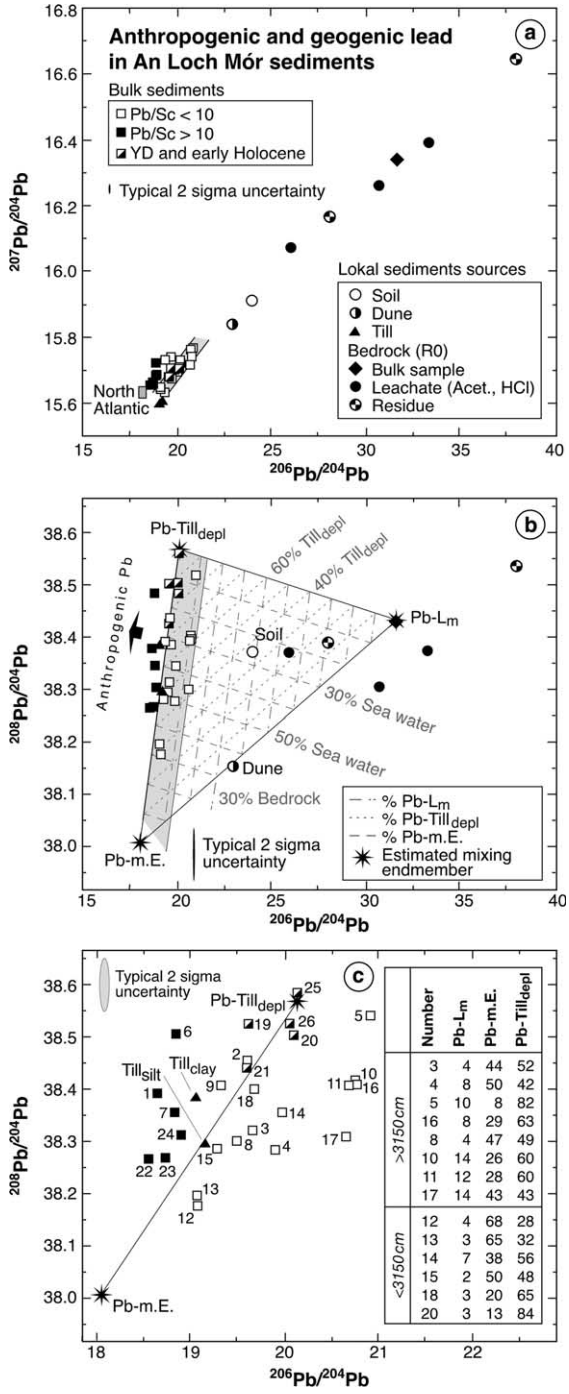

Fig. 4. Pb-isotope data (Tables 2 and 3) of An Loch Mór sediments and potential local sediment sources. (a) and (b) The Pb trend of the lake sediments is defined using samples with Pb/Sc < 10. Sample numbers are given in (c). Grid in (b) shows the relative contribution of 3 end members: Pb from seawater (Pb-m.E.), depleted Till (Pb-$Till_{depl}$), and bedrock (Pb-L_m). Inset Table in (c): end member contributions for selected sediment samples in %.

Soils. The total Pb concentrations of 4 local calcareous soil samples ($CaCO_3$: 84.1–95.3 wt%) vary between 1.8 and 5.8 ppm. There is a positive correlation between Pb and Al_2O_3 (Al_2O_3: 0.16–0.81 wt%). The portion of Pb that is related to unweathered bedrock particles (L_m) is estimated by mass balance

considering the total Pb concentration of L_m (Pb = 0.66 ppm). It varies between 65% and 90%. The Pb/Al_2O_3 (ppm/wt%) values of the balanced non-calcareous soil fractions are between 5.2 and 7.3. The excess Pb in the siliciclastic fraction of the recent soils relative to shale R5 or Mean Continental Crust composition (MCC) may originate from several reservoirs: (1) Residual Pb from the chemical dissolution of calcareous particles (bedrock lithoclasts and marine calcareous bioclasts), (2) seawater-Pb originating from sea spray or seaweed, and (3) anthropogenic Pb from atmospheric deposition. Sample S5, which is closest to mean soil composition, was selected for Pb-isotope analyses. The Pb isotopic composition of the soil falls between the trend for the lake sediments and the trend defined by the bedrock and the sand dune samples (Fig. 4).

Till. Glacial deposits related to the south-west directed ice advance, which reached the Aran Islands during the last glacial maximum, were recovered from a drumlin at Silverstrand near Galway (Fig. 1). These deposits are highly calcareous due to glacial erosion of Carboniferous limestone. The $CaCO_3$ content of the silt-fraction ($Till_{silt}$) is 76.1 wt%, that of the clay fraction ($Till_{clay}$) is 81.4 wt%. The portion of Pb that is not bound to limestone particles is estimated by mass balance in the same way as for the calcareous soil samples. The Pb concentration of the mean bedrock (L_m) is considered as the calcareous component. The portion of non-calcareous Pb of $Till_{silt}$ (6.6 ppm) is 92%, that of $Till_{clay}$ (Pb = 19.5 ppm) 97% (Table 1). Relative to the shale sample R5 (Pb/Al_2O_3 = 1.7) or MCC (Pb/Al_2O_3 = 1.2), the non-calcareous component of fine grain-size fractions of the drift ($^{silic}Till_{silt}$ and $^{silic}Till_{clay}$) shows an enrichment of Pb against Al, which is documented by their Pb/Al_2O_3 values ($^{silic}Till_{silt}$ = 3.4, $^{silic}Till_{silt}$ = 5.0). This geochemical signature of the siliciclastic Till fraction should originate from the enrichment of Pb by chemical limestone dissolution, scavenging of lead from silicate-weathering solutions, and from the atmospheric input of Pb via deposition of sea spray aerosols on the ice sheet (see data for aerosol characteristics from a monitoring site c. 30 km NW of Inish Oírr, Jennings et al., 1991; McGovern et al., 1994). The high portion of HCl-leachable Pb in $Till_{clay}$ (67%) confirms such a hydrogenic signature of the fine drift deposits (see Appendix for explanation of 'hydrogenic'). The Pb isotopic compositions of $Till_{silt}$ and $Till_{clay}$ are similar and fall on the mixing trend of the lake sediments (Fig. 4).

4.2. Lead in the An Loch Mór sediments

4.2.1. Total lead

Total Pb of the An Loch Mór sedimentation record shows enhanced concentrations in its lowermost part (below 3340 cm [>8000 cal. BP], Sections I and II, Fig. 3). The Pb contents decrease continuously with the decline of Al_2O_3, except for enhanced Pb contents at 2710 cm and in the uppermost 50 cm of the sedimentation record. Normalisation with the conservative major element Al removes the Pb anomaly of the lowermost part of the record, whereas the Pb peaks at ~2710 cm and at around 2270 cm remain (Fig. 3).

Climate change at the YD/Holocene transition is reflected by the Pb/Al_2O_3 increase that documents enhanced influx of dissolved Pb for increased drainage from the catchment of the lake. There are a number of less pronounced Pb peaks (2.5-times above background) in the Pb/Al_2O_3 profile that may reflect higher influx of dissolved Pb (Fig. 3). Dissolved elemental influx is quantifiable by geochemical mass balance. A substantial portion of the calculated dissolved elemental influx may not be related to direct dissolved influx, but may originate from the influx of solid particles enriched in trace elements. Dried sea spray aerosols might be an important contributor to the pronounced hydrogenic signatures of the An Loch Mór sediments.

Holocene sediment accumulation in An Loch Mór was largely determined by the net accumulation of autochthonous organic matter and calcite; detrital influx was minor. A geochemical characteristic of the Holocene An Loch Mór sediments is the distinct enrichment of trace elements against the conservative major element Al in comparison to the clastic YD sediments. Some sediment sections show distinct increases of trace elements relative to Al_2O_3 (e.g. $^{exc}Sc(n)\%$, $^{exc}Y(n)\%$ with particularly pronounced peaks at 3150 and 2670 cm, Fig. 3) reflecting enhanced contributions from the dissolved influx. The portion of dissolved influx of Y, Sc, and Pb reaches a similar order of magnitude (Fig. 3) and was distinctly enhanced around 5000 cal. BP and 400 AD when woodland recovery in company with dry climatic conditions favoured a high infiltration rate of seawater (Schettler et al., submitted). Therefore, it is concluded that the contribution of seawater (including the sea spray deposit in the catchment of the lake) to the dissolved influx of Sc, Y and Pb dominates over that of the freshwater discharge from the catchment of the lake.

The enrichment of trace elements in the An Loch Mór sediments is estimated by normalisation using the conservative major element Al. The relative enrichment of Pb in the An Loch Mór sediments falls between that of Sc and Y (Fig. 3). For the detection of excess anthropogenic Pb, natural variations of the bulk siliciclastic and dissolved influx of Pb are therefore most adequately considered if Sc or Y are used for normalisation. The background value for Pb/Sc in the An Loch Mór sediments shows a slight increase, but remains in the same order of magnitude (2–5) throughout the Holocene although major variations in the autochthonous sedimentation are indicated from geochemical element profiles (Fig. 3). There are several sections showing Pb/Sc ratios clearly above the background, most prominently at 2270 and 2710 cm depth. The anomaly at 2270 cm is related to increased input of anthropogenic Pb during modern industrial history, whereas the Pb peak at 2710 cm originates from Pb emissions at ancient mining sites.

4.2.2. Lead isotope composition

The $^{206}Pb/^{204}Pb$ ratio of the sediment samples ranges between 18.63 and 20.89 (Table 3). The data define a linear trend in both the $^{206}Pb/^{204}Pb$–$^{207}Pb/^{204}Pb$ and the $^{206}Pb/^{204}Pb$–$^{208}Pb/^{204}Pb$ diagram (Fig. 4a,b), which could be obtained by the mixing of two isotopically different Pb components in various proportions. Scattering along this trend may reflect analytical uncertainty along with minor contributions from additional Pb reservoirs. YD sediments (samples: 25 and 26, Fig. 4) are characterised by relatively high $^{208}Pb/^{204}Pb$ values (Table 3, Fig. 4). They could represent the thorogenic end member of the mixing line. Samples 12 and 13 have the lowest $^{208}Pb/^{204}Pb$ values. These two samples have been deposited after the onset of diurnal seawater infiltration when diurnal infiltration of seawater was favoured by dry climatic conditions and regeneration of woody vegetation in the catchment of the lake (Schettler et al., submitted). Sediment samples of this section are characterised by a distinct enrichment

Table 3
Lead isotopic composition, bulk Pb, and selected geochemical parameters of An Loch Mór sediments

	Sample[a] (TIMS)	Depth (cm)	$\frac{^{206}Pb}{^{204}Pb}$[b]	$\frac{^{207}Pb}{^{204}Pb}$[b]	$\frac{^{208}Pb}{^{204}Pb}$[b]	$\frac{^{208}Pb}{^{206}Pb}$[b]	Pb (ppm)	Al_2O_3 (wt%)	Pb/Al_2O_3 (ppm/wt%)	^{exc}Pb(total)[c]	
										(ppm)	%
1	MOR1-Ia-30	2273.5	18.634	15.664	38.392	2.0603	30.1	0.69	43.5	27.9	(92.7)
2	MOR1-Ib-41.5	2385.5	19.591	15.741	38.455	1.9629	8.5	0.79	10.7	5.98	(70.3)
3	MOR1-Ib-45.5	2389.5	19.623	15.701	38.321	1.9529	7.4	0.77	9.62	4.96	(67.0)
4	MOR1-IIa-92.5	2545.5	19.891	15.701	38.283	1.9246	5.7	0.80	7.11	3.11	(55.0)
5	MOR2-IIb-21.5	2680.5	20.894	15.782	38.541	1.8446	4.0	0.81	4.9	1.40	(35.2)
6	MOR1-IIIa-33.5	2698.5	18.843	15.722	38.505	2.0435	22.3	0.93	23.9	19.3	(86.7)
7	MOR1-IIIa-41.5	2706.5	18.805	15.684	38.357	2.0397	35.7	1.10	32.4	32.2	(90.2)
8	MOR1-IIIa-77.5	2742.5	19.482	15.685	38.301	1.9660	8.0	0.80	9.96	5.45	(68.1)
9	MOR1-IVa-57.5	2931.5	19.311	15.730	38.408	1.9889	15.3	0.96	15.9	12.2	(80.0)
10	MOR1-IVa-81.5	2955.5	20.739	15.767	38.418	1.8525	3.5	0.73	4.77	1.18	(33.6)
11	MOR2-IVa-101.5	3086.5	20.665	15.761	38.408	1.8586	7.1	0.95	7.44	4.07	(57.3)
12	MOR1-Va-67.5	3153.5	19.085	15.643	38.178	2.0004	5.6	0.50	11.2	3.99	(71.5)
13	MOR1-Va-71.5	3157.5	19.040	15.645	38.198	2.0062	5.2	0.46	11.3	3.71	(71.7)
14	MOR1-VIa-108.5	3405.5	19.957	15.698	38.355	1.9219	23.7	3.68	6.43	12.0	(50.5)
15	MOR1-VIa-112.5	3409.5	19.276	15.637	38.286	1.9862	21.3	3.68	5.78	9.62	(45.2)
16	MOR2-IIa-118.5	2676.5	20.749	15.743	38.411	1.8512	4.06	0.81	5.01	2.03	(50.0)
17	MOR1-Va-55.5	3141.5	20.625	15.716	38.308	1.8574	6.2	1.12	5.55	2.64	(42.7)
18	MOR1-VIb-33.5	3431.0	19.676	15.675	38.399	1.9516	25.8	6.92	3.73	3.87	(15.0)
19	MOR1-VIb-53.5	3451.0	19.606	15.703	38.525	1.9650	32.0	9.84	3.25	0.74	(2.3)
20	MOR1-VIb-57.5	3455.0	20.083	15.704	38.506	1.9173	31.7	10.11	3.14	−0.41	(–)
21	MOR1-VIb-73.5	3471.0	19.584	15.675	38.442	1.9629	14.7	6.63	2.22	−6.34	(–)
22	MOR1-IIIa-38(s)	2703	18.560	15.657	38.268	2.0619	38.2	0.95	40.2	22.6	91
23	MOR1-IIIa-43(s)	2708	18.729	15.660	38.270	2.0434	38.6	1.17	33.0	23.1	89
24	MOR1-IIIa-58(s)	2723	18.899	15.687	38.312	2.0272	28.4	1.16	24.5	3.7	56
25	MOR1-VIb-76(s)	3473	20.109	15.725	38.587	1.9189	17.6	6.77	2.60	–	(–)
26	MOR1-VIb-77(s)	3474	20.050	15.706	38.526	1.9215	16.8	6.35	2.65	–	(–)

[a] Sample name composed of drill site (MOR1 or MOR2), core number, and position within the core. Samples marked with (s) represent 1 cm sections, other samples represent re-mixed 1 cm samples representative for 4 cm sections. Actual depth of the sample mid-point is given in centimeter with reference to the lake surface. Position of TIMS-samples 1 through 26 is shown in Figs. 2 and 4, respectively.

[b] Analytical procedure and precision as in Romer et al. (2001).

[c] ^{exc}Pb(total) calculated for $Pb/Al_2O_3 = 2.5$ (ppm/wt%).

of Y, Pb and Sc (Fig. 3), which should largely originate from dissolved influx via seawater input. The prolongation of this mixing trend towards low $^{208}Pb/^{204}Pb$ should pass through seawater Pb. Hence, the intersection of this mixing trend with the trend defined by the bedrock and dune-Pb estimates the Pb isotopic composition of seawater (Fig. 4).

$Till_{silt}$ and $Till_{clay}$ samples show a higher enrichment of Pb versus the major element Al than the clastic YD sediments (Table 1). The excess Pb component in the fine fraction of the regional drift might be characterised by a low radiogenic composition as derived for seawater Pb and may document the aeolian deposition of sea spray aerosols over western Ireland. Lead originating from sea-salt aerosols is weakly bound and is leached during till weathering, which could explain the shift of the clastic late YD sediment samples towards lower radiogenic composition. The hypothetical radiogenic end member is therefore termed depleted till ($Till_{depl}$).

Sediment samples 1, 6, 7, 22, 23 and 24 correspond to distinct Pb/Sc peaks at 2270 and 2710 cm depth, sample 9 represents sediments with a less pronounced Pb/Sc peak at 2935 cm (Fig. 3). Omission of these samples improves the linear trend of the sediment samples in the $^{206}Pb/^{204}Pb$– $^{207}Pb/^{204}Pb$ and the $^{206}Pb/^{204}Pb$–$^{208}Pb/^{204}Pb$ diagrams. All samples with enhanced Pb/Sc ratios fall to the left of this trend (Fig. 4).

The relative contributions of the 3 Pb end members Pb–m.E., Pb-$Till_{depl.}$, and Pb-L_m in selected Holocene sediment samples with Pb/Sc < 10 has been calculated by simple Pb isotope mass balance (Inset Table, Fig. 4). Siliciclastic Pb (Pb-$Till_{depl}$) represents the major constituent in all balanced samples; there are substantial contributions from Pb-m.E., whereas the contents of uranogenic bedrock Pb (Pb-L_m) are only minor.

5. Discussion

5.1. Ancient mining and processing of Pb ores

Extensive ancient mining of Pb ores must be seen in the context of the production of Ag, which was needed in increasing amounts by the spread of coinage after c. 500 BC. The cupellation of Pb–Ag alloys formed by roasting of argentiferous Pb ores is a metallurgical technology, which was already known in early cultures (Nriagu, 1993). During cupellation, liquid Ag is separated from solid Pb-oxides by the oxidation of molten Pb at temperatures above 1000 °C. There is evidence for significant Ag production in Spain as early as during the 7th and 8th century BC favoured by Phoenician trading (cf. Nriagu, 1993; Shepherd, 1993) and for even earlier mining of argentiferous Pb ores at Rio Tinto (Spain) (1100–800 BC, e.g. Shepherd, 1993). Extensive Ag production, furthermore, is documented for Laurion (Greece) from 600 BC to 300 BC with a peak around 490–480 BC due to the financial efforts made by the Athenians to defend against Xerxes' campaign (Shepherd, 1993). Similarly, exploitation of argentiferous Pb ores by the Carthaginians in Spain has to be seen in the context of the financial efforts for the Second Punic War (218–201 BC, Shepherd, 1993). Mining of Pb ores and related atmospheric pollution reached its maximum in the Roman period and is certainly related to the metallurgical processing of argentiferous Pb ores. Ancient Ag production may have reached a maximum of 30×10^3 tons between 50 BC and AD 100, whereas production in the 100 a before and after, respectively, is estimated to have been in the range of 10×10^3 tons (Patterson, 1972). Historical and archaeological data suggest that mining of Pb and Ag was most intense from 75 BC to AD 170 (see Nriagu, 1993; Shepherd, 1993), the most productive mines being located on the Iberian Peninsula and after AD 43 in the British Isles (Mendips of Somerset, Shropshire, Derbyshire, the Pennines, and Cornwall).

There are several major Pb–Zn ore deposits in the Irish Midlands (Andrew et al., 1986), the largest ones are Navan (>70 Mt), Lisheen (>20 Mt), and Silvermines (>17.7Mt) (Johnston, 1999). Mining of these deposits generally started after the mid-1960s (O'Brien, 2004, p. 38). There is archaeological evidence for an important centre of pre-medieval metal-working in SW Ireland near Killarney town, Co. Kerry. Mining of polymetallic deposits for Cu started c. 2500 BC in the region. Metal tools produced from Cu of these deposits are identifiable by their high As, Sb and Ag contents that originate from the smelting of fahlerz Cu ores (O'Brien, 2004 and references therein). As Pb minerals are typical constituents in the polymetallic mineral deposits of SW Ireland, there may have been Pb-emissions associated with Cu ore processing. The mining for Cu declined with the widespread adoption of Fe metallurgy in Ireland around 300 BC. Non-ferrous metals were used almost exclusively in the manufacture of luxury items afterwards. There is no archaeological evi-

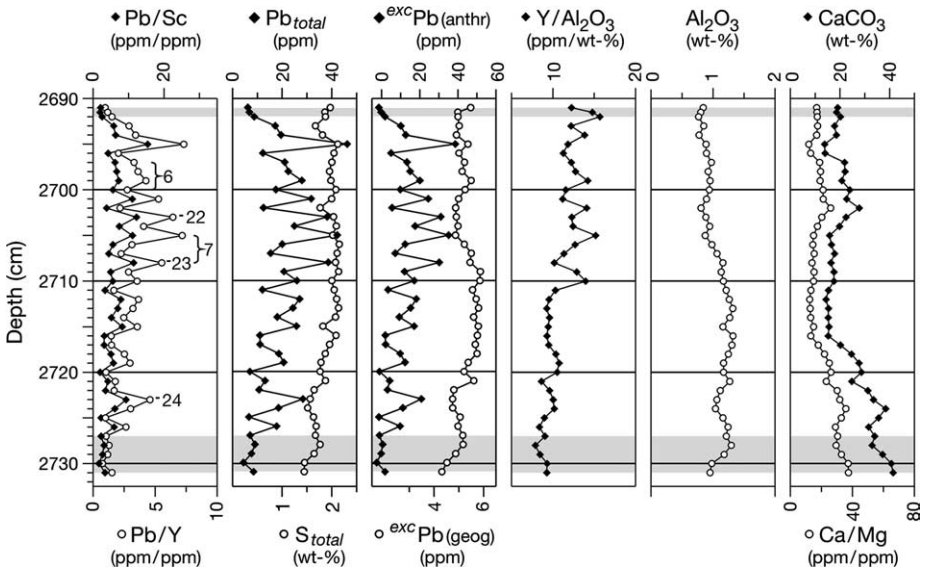

Fig. 5. Highly resolved geochemical sediment-profiles of the An Loch Mór sediment-section that documents enhanced atmospheric influx of Roman-Pb. Each 1-cm sample represents c. 5 a. Numbers inside the diagram document the position of individual TIMS-samples. Shading in the upper and lower part of the Pb/Sc-profile mark the samples used for the definition of the Pb/Sc and Pb/Y background values. The decrease of $CaCO_3$ and Ca/Mg documents decreasing inflow of freshwater in the upper part of the section. The anthropogenic Pb excess ^{exc}Pb(anthr) is calculated by geochemical mass balance using a Pb/Sc value of 4.2 [ppm/ppm]. The geogenic Pb excess ^{exc}Pb(geog) is calculated as difference ^{exc}Pb(total)–^{exc}Pb(anthr) (see Table 5).

dence for the cuppelation of Ag from Pb ores in the region (O'Brien, 2004).

5.2. Identification and quantification of anthropogenic Roman Pb in An Loch Mór sediments

Fig. 5 shows the Pb record and major geochemical signatures of sediments between 2691 and 2731 cm (c. AD 250–AD 50) at 1 cm sample resolution. Individual TIMS-samples are marked inside the diagram. Each 1-cm sample represents approximately 5 a. Diffusive transport of dissolved Pb in pore water (equilibrated with adsorbed Pb) may proceed if the Pb concentration gradients are maintained for longer periods by H_2S generation and sulphide precipitation within the surface sediments. There is no indication of diffusive redistribution of Pb by coinciding maxima of Pb_{total} and S_{total} in the sediment section between 2691 and 2731 cm (Fig. 5).

Detailed geochemical mass balance data for sediments between 2691 and 2731 cm are given in Table 4. The portion of Pb that does not originate from geogenic siliciclastic (detrital) influx [^{exc}Pb(total)] is estimated by chemical mass balance using the average Pb/Al_2O_3 of late YD-sediments as a reference for the chemical composition of the siliciclastic input (2.5 [ppm/wt%]). Between 2691 and 2731 cm, the Pb-excess accounts for 50% and 90% in total Pb [^{exc}Pb(r)] and is positively correlated with the total Pb concentration.

Normalisation with Sc slightly over-estimates the natural dissolved influx of Pb, whereas normalisation with Y tends to result in an under-estimation of the dissolved Pb-influx (Section 4.2.1.). Lead-peaks that remain after normalisation with Sc and Y reflect input of anthropogenic Pb (Fig. 5). Lead/Sc-maxima coincide with Y/Al_2O_3-peaks at various depths (2699, 2705, 2710, 2719, 2723 cm), but, there are also sediment sections with Pb/Sc-peaks (2695, 2701, 2703, 2708, 2712, 2715, 2726 cm) that do not show a coinciding increase of Y/Al_2O_3. Since a general correlation between Pb/Sc (Pb/Y) and Y/Al_2O_3 does not exist, it is concluded that seawater is unlikely to be the general carrier for the influx of anthropogenic Pb.

The Pb/Sc and Pb/Y background values, as estimated from the chemical composition of adjoining sediments above and below the contaminated sediment interval, are 4.2 and 0.71 (Fig. 5, Table 4). Based on these values, the concentration of the anthropogenic Pb component [$^{exc}Pb^{Sc}$(anthr) and $^{exc}Pb^{Y}$(anthr), respectively] is estimated by mass balance. The mean $^{exc}Pb^{Sc}$(anthr) concentration between 2693 and 2726 cm is 13.4 ppm. Geochemical mass balance based on Pb/Y gives a mean anthropogenic Pb content of 13.0 ppm (Table 4).

Table 4
Selected geochemical parameters of An Loch Mór sediments contaminated by Roman Pb

Sample	Depth (cm)	Al_2O_3 (wt%)	Sc (ppm)	Y (ppm)	Pb_{total} (ppm)	Pb/Sc (ppm/ppm)	Pb/Y (ppm/ppm)	^{exc}Pb(total)[a] (ppm)	^{exc}Pb(r) (%)	Pb_{anthr}[b]			Pb(geog)[c]		^{exc}Pb (geog)[d]	
										$^{exc}Pb^{Sc}$[h] (ppm)	$^{exc}Pb^{Y}$[h] (ppm)	$^{exc}Pb^{Sc}$[h] (%)	[Sc][h]		[Sc][h]	
													ppm	$\%_{silic}$[e]	ppm	%
Mor2-IIb-32[f]	2691	0.843	1.81	10.3	6.00	3.4	0.60	4.1	66				6.00	8	5.5	92
Mor2-IIb-33[f]	2691.5	0.804	1.66	11.9	6.84	4.1	0.57	4.8	71				6.84	27	5.0	73
Mor1-IIIa-27[f]	2692	0.768	1.64	12.1	8.76	5.3	0.73	6.8	78				8.76	43	5.0	57
Mor1-IIIa-28	2693	0.852	1.70	10.4	17.3	10	1.67	15.2	88	10.2	9.9	67	7.1	43	5.0	29
Mor1-IIIa-29	2694	0.777	1.63	10.7	19.6	12	1.82	17.7	90	12.8	12.0	72	6.8	40	4.9	25
Mor1-IIIa-30	2695	0.888	1.81	10.5	46.3	26	4.41	44.1	95	38.7	38.9	88	7.6	41	5.4	12
Mor1-IIIa-31	2696	0.897	1.73	10.1	12.3	7.1	1.22	10.1	82	5.1	5.1	50	7.2	45	5.0	41
Mor1-IIIa-32(TIMS-6)	2697	0.976	1.83	12.0	21.1	12	1.76	18.7	88	13.4	12.6	72	7.5	48	5.2	25
Mor1-IIIa-33(TIMS-6)	2698	0.925	1.77	11.8	22.5	13	1.91	20.2	90	15.1	14.1	75	7.0	46	5.1	23
Mor1-IIIa-34(TIMS-6)	2699	0.954	1.88	13.6	28.0	15	2.06	25.6	92	20.1	18.4	79	7.9	43	5.5	20
Mor1-IIIa-35(TIMS-6)	2700	0.942	1.81	10.9	17.5	9.7	1.61	15.2	87	9.9	9.8	65	7.6	44	5.3	30
Mixed(6)[g]	*2699*	*0.896*	*1.86*	*11.6*	*22.3*	*12*	*1.92*	*29.6*	*93*	*14.5*	*14.1*	*73*	*7.8*	45	*5.5*	*25*
Mor1-IIIa-36	2701	0.810	1.72	10.0	31.8	19	3.17	10.5	84	24.6	24.7	83	7.2	41	5.0	16
Mor1-IIIa-37	2702	0.885	1.64	11.4	12.5	7.6	1.09	36.0	94	5.6	4.4	54	6.9	45	4.9	39
Mor1-IIIa-38(TIMS-22)	2703	0.949	1.69	10.9	38.2	23	3.51	22.6	91	31.1	30.5	86	7.1	47	4.9	13
Mor1-IIIa-39	2704	0.877	1.75	11.8	25.0	14	2.12	40.1	95	17.7	16.6	78	7.3	44	5.0	20
Mor1-IIIa-40(TIMS-7)	2705	0.983	1.68	13.3	42.3	25	3.18	17.7	88	35.2	32.9	88	7.1	48	4.9	12
Mor1-IIIa-41(TIMS-7)	2706	1.07	1.83	12.5	20.1	11	1.61	12.7	83	12.4	11.2	70	7.7	49	5.2	26
Mor1-IIIa-42(TIMS-7)	2707	1.16	1.95	12.1	15.4	7.9	1.27	35.7	93	7.2	6.8	57	8.2	52	5.5	36
Mixed(7) [g]	*2707*	*1.13*	*2.04*	*13.3*	*35.7*	*18*	*2.69*	*17.9*	*86*	*27.1*	*26.3*	*82*	*8.6*	48	*5.8*	*16*
Mor1-IIIa-43(TIMS-7-23)	2708	1.17	1.99	11.8	38.6	19	3.26	23.1	89	30.3	30.2	85	8.3	49	5.5	14
Mor1-IIIa-44	2709	1.21	2.07	14.6	20.8	10	1.42	9.0	75	12.1	10.4	67	8.7	53	5.9	28
Mor1-IIIa-45	2710	1.26	2.09	16.3	26.0	13	1.59	24.0	88	17.2	14.4	75	8.8	55	5.9	23
Mor1-IIIa-46	2711	1.32	2.05	12.5	12.1	5.9	0.96	21.1	87	3.5	3.2	39	8.6	57	5.6	46
Mor1-IIIa-47	2712	1.27	2.11	12.0	27.1	13	2.25	14.9	82	18.3	18.6	76	8.8	57	5.7	21

Mor1-IIIa-48	2713	1.16	2.17	12.3	24.4	11	1.99	22.9	89	15.3	15.7	73	9.1	50	5.8	24
Mor1-IIIa-49	2714	1.32	2.09	12.2	18.1	8.7	1.48	7.8	70	9.3	9.4	63	8.8	56	5.6	31
Mor1-IIIa-50	2715	1.31	2.07	11.0	25.8	13	2.35	7.9	71	17.1	18.0	75	8.7	57	5.8	23
Mor1-IIIa-51	2716	1.25	2.16	12.3	11.1	5.2	0.90	15.6	83	2.1	2.4	26	9.1	55	5.8	52
Mor1-IIIa-52	2717	1.17	2.13	12.4	11.2	5.2	0.90	17.7	86	2.2	2.3	28	9.0	54	5.7	51
Mor1-IIIa-53	2718	1.17	2.11	12.9	18.7	8.9	1.45	4.1	59	9.9	9.5	63	8.8	57	5.7	31
Mor1-IIIa-54	2719	1.27	1.98	12.6	20.7	10	1.64	9.9	76	12.4	11.7	70	8.3	57	5.4	26
Mor1-IIIa-55	2720	1.12	1.94	12.3	7.05	3.6	0.57	8.0	74	–	–	–	7.05	26	5.2	74
Mor1-IIIa-56	2721	1.06	2.09	11.0	13.1	6.3	1.20	25.8	91	4.3	5.3	44	8.8	54	5.6	43
Mor1-IIIa-57	2722	1.04	1.81	10.8	10.8	6.0	1.00	16.0	86	3.2	3.1	40	7.6	54	4.8	45
Mor1-IIIa-58(TIMS-24)	2723	1.16	1.77	10.7	28.4	16	2.66	3.7	56	21.0	20.8	82	7.4	56	4.8	17
Mor1-IIIa-59	2724	1.25	1.75	10.6	18.6	11	1.75	14.7	83	11.2	11.0	70	7.4	62	4.8	26
Mor1-IIIa-60	2725	1.22	1.89	10.4	6.65	3.5	0.64	4.1	58	–	–	–	6.65	23	5.1	76
Mor1-IIIa-61	2726	1.30	1.92	10.4	17.9	9.3	1.71	5.9	64	9.8	10.4	66	8.1	62	5.0	28
Mor1-IIIa-62[f]	2727	1.18	1.95	11.0	7.18	3.7	0.65	4.7	62				7.18	28	5.2	72
Mor1-IIIa-63[f]	2728	0.980	2.00	10.2	9.10	4.5	0.89	2.0	45				9.10	43	5.2	57
Mor1-IIIa-64[f]	2729	0.953	1.86	10.0	7.70	4.1	0.77	6.2	72				7.70	56	4.9	64
Mor1-IIIa-65[f]	2730	0.931	1.66	9.1	4.45	2.7	0.49	20.0	90				4.45	–	4.5	102
Mor1-IIIa-66[f]	2731	1.10	1.60	8.8	8.54	5.4	0.97	32.9	92				8.54	49	4.3	51

[a] Difference between Pb_{total} and Pb_{silic} is calculated using $Pb/Al_2O_3 = 2.5$ (ppm/wt%). $^{exc}Pb(r)$ is calculated as percentage of Pb_{total}.

[b] Geogenic Pb-input is estimated using Pb/Sc and Pb/Y. The values of these parameters are defined from 8 background samples taken directly above and below the anomalous section (Pb/Sc = 4.2 and Pb/Y = 0.71). Pb(anthr) is calculated for Pb/Sc and Pb/Y background values of 4.2 and 0.71, respectively. The percentage of Pb(anthr) is calculated relative to $^{exc}Pb(total)$. For a sedimentation rate of 1.95 mm/a, a density of the dried sediment of 1.8 g/cm^3, and a porosity of 0.5, there is an average $^{exc}Pb(anthr)$-flux into the lake of 24.3 (23.5) mg m^{-2} a^{-1} over a period of 169 a. $^{exc}Pb(anthr)$–flux calculated for Pb/Sc = 4.2, value in brackets for Pb/Y = 0.71.

[c] The content of geogenic Pb represents the difference between Pb(total) and $^{exc}Pb(anthr)$ calculated on the basis of Pb/Sc.

[d] $^{exc}Pb(geog) = {}^{exc}Pb(total) - {}^{exc}Pb(anthr)$ on the basis of (Pb/Sc). Percentage of $^{exc}Pb(geog)$ is given relative to Pb_{total}.

[e] Percentage of Pb_{silic} in geogenic Pb. $\%Pb_{silic} = 100 \cdot [Pb(geog) - {}^{exc}Pb(geog)]/Pb(geog)$

[f] Samples used to define the background values for Pb/Sc and Pb/Y, respectively.

[g] Individual samples used to prepare the mixed TIMS-samples 6 and 7, respectively, are marked behind the sample name.

[h] [Sc]: anthropogenic Pb contribution calculated for a background value of Pb/Sc = 4.2; [Y]: anthropogenic Pb contribution calculated for a background value of Pb/Y = 0.71.

Table 5
Combined geochemical and Pb isotope mass balance

TIMS-sample	Pb_{total} (ppm)	^{exc}Pb(geog)		Pb_{silic}(geog)	^{exc}Pb(anthr) (ppm)	Calculated Pb_{anthr}		
		Pb-L_m (ppm)	Pb-m.E. (ppm)	Pb-$Till_{depl}$		$^{206}Pb/^{204}Pb$	$^{207}Pb/^{204}Pb$	$^{208}Pb/^{204}Pb$
Samples with anthropogenic Pb (Pb/Sc > 10)								
6	22.3	0.69	4.8	2.33	14.5	18.39	15.73	38.7
6*						18.26	15.73	38.6
6**						18.30	15.73	38.6
22	38.2	0.61	4.29	2.21	31.1	18.25	15.65	38.2
7	35.7	0.72	5.07	12.76	27.1	18.44	15.68	38.3
23	38.6	0.68	4.77	2.9	30.3	18.38	15.65	38.2
24	28.4	0.59	4.16	2.66	21.0	18.51	15.68	38.3
Samples with Pb/Sc < 10								
				Pb_{silic}(geog)		Calculated Pb_{silic}(geog)		
				Variable (ppm)	m.E./L_m	$^{206}Pb/^{204}Pb$	$^{207}Pb/^{204}Pb$	$^{208}Pb/^{204}Pb$
Above 3170 cm (after c. 5500 cal. BP)								
2	8.46	0.42	6.05	1.99	14	22.2	16	40
3	7.43	0.47	5.04	1.92	11	21.3	15.76	39.2
4	5.65	0.41	3.77	1.46	9	19.9	15.66	38.7
5	3.98	0.58	1.45	1.95	3	20.3	15.76	39
16	4.06	0.58	1.45	2.03	2	20.1	15.68	38.7
8	8.02	0.48	5.53	2.01	12	21	15.71	39.2
8*						20.3	15.69	38.9
8**						19.9	15.68	38.7
9	15.3	0.64	12.1	2.53	19	22.9	16.12	40.6
10	3.5	0.49	1.18	1.83	2	20	15.73	38.7
11	8.59	1.28	3.29	4.02	3	19.9	15.72	38.8
17	6.18	0.93	2.46	2.79	3	19.8	15.61	38.6
12	5.58	0.17	4.16	1.25	24	21	15.56	38.7
13	5.17	0.16	3.86	1.15	24	20.8	15.62	38.9
Below 3170 cm								
14	23.7	2.23	12.4	9.1	6	20.1	15.66	38.8
15	21.3	0.48	11.6	9.2	14	20.3	15.61	38.7
18	25.8	0.12	5.84	19.8	49	20.3	15.69	38.6
19	32	0.22	7.17	24.6	32	20	15.72	38.7
20	31.7	0.38	6.03	25.3	16	20.4	15.71	38.6

Calculation of the Pb isotopic composition of samples 6*, 6**, 8*, and 8** as for Figs. 5 and 6.

The balanced content of anthropogenic Pb [^{exc}Pb(anthr)] is highly variable, it rises up to 88% of ^{exc}Pb(total) and shows distinct minima in periods of about 20–30 a (Fig. 5).

5.3. Lead isotope composition of anthropogenic Roman Pb in An Loch Mór sediments

The isotopic composition of Roman Pb contamination (Pb_{anthr}) between 2693 and 2726 cm is estimated by combined bulk-geochemical and Pb-isotopic mass balance for selected sediment samples (TIMS-samples: 6, 22, 7, 23, and 24, see Fig. 5, and Tables 4 and 5) in the following way. The geogenic Pb excess [^{exc}Pb(geog)], which estimates the natural influx of dissolved Pb, is calculated as the difference of ^{exc}Pb(total) and $^{exc}Pb^{Sc}$(anthr), the siliciclastic Pb component (Pb_{silic}) is calculated by $Pb_{total}-{}^{exc}Pb$(total) (Table 4). For the balanced TIMS-samples 6, 22, 7, 23, and 24, the contribution of ^{exc}Pb(geog) to Pb_{total} varies between 13% and 25%, and the portion of Pb_{silic} to Pb_{total} between 6% and 10%. The excess anthropogenic Pb [^{exc}Pb(anthr)] is the major Pb constituent in the balanced TIMS-samples (65–81%, Table 5). For the estimation of the isotope composition of ^{exc}Pb(anthr) by isotope mass balance, two geogenic components are considered: siliciclastic Pb (Pb_{silic}) and ^{exc}Pb(geog), which is represented by a mixture of the two end members seawater Pb (Pb–m.E.) and local limestone Pb (Pb-L_m).

In a first approach, it is assumed that the siliciclastic Pb component (Pb_{silic}) is closely represented by that of the clastic YD-sediments ($Till_{depl}$). The Al_2O_3 concentrations in the An Loch Mór sediments

have been sustained on a level of about 1 wt% over the last 7 ka. The Al_2O_3 content of the An Loch Mór sediments cannot originate from the influx of local calcareous materials of the modern island which have Al_2O_3 concentrations distinctly below 1 wt% (Table 1). It is likely that the lake receives siliciclastic input via influx of sea spray aerosols. Galway Bay receives substantial particle influx by terrestrial run-off (mean discharge Lough Corrib [Fig. 1]: 83 $m^3 s^{-1}$) and by coastal erosion of drumlin deposits. Suspended material in Galway Bay, therefore should show similar geochemical and Pb isotope signatures as the fine grain-size fractions of regional drift. However, the isotopic signatures of weakly bound Pb of seawater suspended particles may be modified by exchange with seawater dissolved Pb.

The Pb-m.E./Pb-L_m ratio has been higher during early Holocene periods, without human impact on local vegetation and a generally lower freshwater discharge from the catchment of the lake. For TIMS-samples above and below the polluted sediment section (2693–2726 cm), the balance between Pb-m.E. and Pb-L_m in ^{exc}Pb(geog) is about 2.5 (TIMS-samples 5 and 16) and 12 (TIMS-sample 8), respectively (Fig. 3, Table 5). For the determination of the Roman Pb by Pb isotopic mass balance, a constant seawater-Pb to bedrock-Pb ratio of 7 is used. Higher bedrock-Pb contributions shift the derived anthropogenic Pb components ($Pb_{anthr}[i]$) towards lower $^{206}Pb/^{204}Pb$ values, but has only minor influence on the $^{208}Pb/^{204}Pb$ values of ($Pb_{anthr}[i]$).

In a second approach, we consider that the provenance of the siliciclastic influx varied during the Holocene, which is supported by the decrease of Al/Ti (Fig. 3). Aeolian influx of remote dust from two major source regions may have increasingly contributed to the bulk siliciclastic influx into Lake An Loch Mór, whereas local till relicts became exhausted by erosion: (i) Desertification of North Africa through climate change from the mid Holocene has been accompanied by increased wind erosion. Generally enhanced aeolian transport of Saharan dust into the North Atlantic after c. 5500 cal. BP has been clearly detected in marine sediment records west of Africa (e.g. DeMenocal et al., 2000). Saharan dust plumes occasionally reach Ireland (e.g. Tullet, 1980, 1984). (ii) Woodland clearance and gradual spread of farming in western Europe from the Neolithic increased wind erosion. Dust from these sources may have been transported to Ireland due to meteorological conditions favouring easterly wind directions.

The isotopic composition of the siliciclastic Pb component (Pb_{silic}) of uncontaminated or relatively little contaminated Holocene sediment samples (Pb/Sc < 10) is estimated by combined bulk-geochemical and Pb isotopic mass balance (Table 5). The Pb isotope composition of the siliciclastic Pb components of TIMS-samples 18, 19 and 20, which represent early Holocene sediments, closely corresponds with that of $Till_{depl}$, whereas the Pb_{silic}-components of younger sediments are generally characterised by a more thorogenic composition. The Pb_{silic}-components of the TIMS-samples 3, 5, and 8, which may characterise the geogenic background of individual sediment samples with anthropogenic Roman Pb, most closely plot in the $^{206}Pb/^{204}Pb$–$^{208}Pb/^{204}Pb$ diagram within a relatively narrow cluster above $Till_{depl}$ (Fig. 7). The isotope composition of the balanced siliciclastic Pb component of TIMS sample 8 ($Pb_{silic}[8]$) was used as end member to balance the isotope composition of Pb_{anthr} of TIMS sample 6. Because of the low contribution from Pb_{silic} (Table 5), the balanced isotopic composition of the anthropogenic Pb component only slightly differs from that of the first approach (Fig. 6).

Contamination of the marine end member by thorogenic Pb from the siliciclastic Pb component would shift the Pb isotope composition of the siliciclastic Pb component of TIMS sample 8 towards a less radiogenic composition (see Fig. 7 for Pb-isotope characteristics of $Pb_{silic}[8]$ with an assumed seawater contamination of 10% and 20%). For these assumptions, the estimated anthropogenic Pb component of TIMS-sample 6 falls between the values from the other two approaches (Fig. 6, Table 5).

5.4. Chronology and sources of ancient Pb pollution in An Loch Mór sediments

The Pb-peak at 2710 cm in the An Loch Mór record (Fig. 3) occurs at the beginning of the so-called Late Iron Age Lull period in Ireland (LIAL: c. AD 100–500). A substantial decline in farming, especially in western Ireland, favoured the regeneration of woodland during this period (e.g. O'Connell, 1994). The pollen record of An Loch Mór documents a distinct spread of woody vegetation (mainly *Juniperus* and *Taxus*) also on Inis Oírr during the LIAL (Molloy and O'Connell, 2004). Enhanced influx of anthropogenic Pb around 2710 cm clearly falls in the time of the Roman Empire. For a constant sedimentation rate of 1.95 mm/a between 0 AD/BC (2741 cm) and the chronomarker T3 (Hekla 1 at 2526 cm, AD

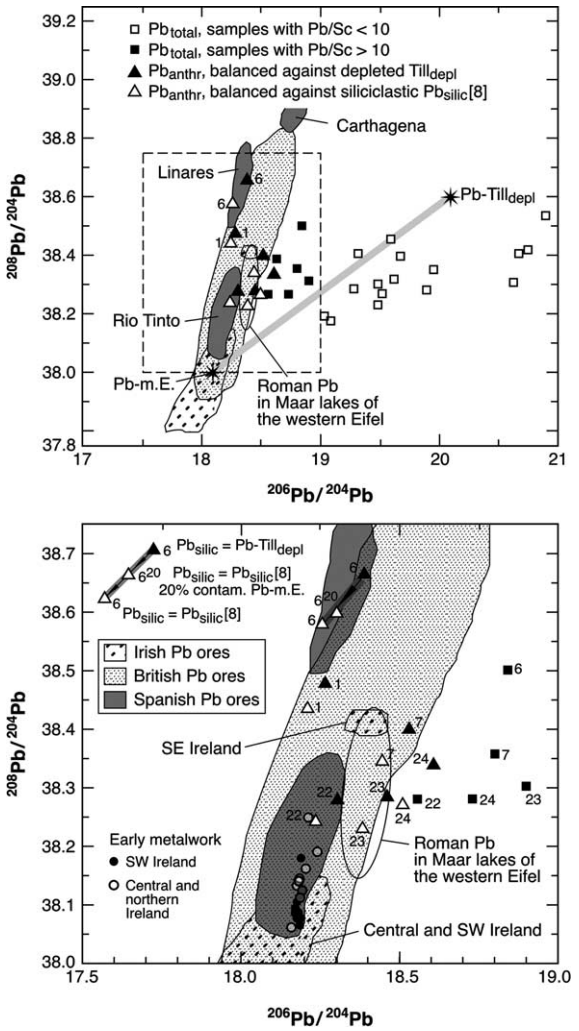

Fig. 6. $^{206}Pb/^{204}Pb$–$^{208}Pb/^{204}Pb$ diagram showing the measured Pb-isotopic composition of the sediment samples (Table 3), the end members (Table 2) used for Pb modelling and the calculated isotopic composition of the anthropogenic Pb. The anthropogenic Pb component is obtained by mass balance using $Till_{depl}$ to account for contributions of the siliciclastic Pb component. As examples, the same mass balance were made for sample 6 using the estimated Pb-isotopic composition of the balanced siliciclastic Pb component of sample 8 $Pb_{silic}[8]$, and assuming additionally 20% contamination of seawater by Pb from $Pb_{silic}[8]$, respectively (see Fig. 6). Fields for Pb ores of Ireland, Britain and Spain are for reference. Note, that the estimated Pb-isotopic composition of the anthropogenic Pb of sample 6 falls in the field of Linares (Spain) and those of samples 7, 22, 23, and 24 fall in or close to the field of Rio Tinto (Spain). The anthropogenic Pb component could as well originate from British mining sites. Data sources for reference fields: Arribas et al. (1991), Dixon et al. (1990), Haggerty et al. (1996), LeHuray et al. (1987), Stos-Gale et al. (1995), and Rohl (1996). Roman Pb in Maar lakes of the western Eifel after Schettler and Romer (1998). Circles: Isotopic composition of Bronze Age metal work given in O'Brien (2004); filled, SW Ireland, primary data Northover et al., 2001; unfilled, Northern and central Ireland, primary data Rohl and Nedham (1998).

1104; Fig. 3) detectable Pb-pollution started at AD 77 and lasted 169 a until AD 246. Sediment accumulation, however, may have varied between 0 BC/AD and AD 1104. In a varved sediment section (Fig. 3), sediment accumulation declined from 1.5 mm/a (3246–3276 cm) to 0.87 mm/a (3173–3246 cm) by reduced net-accumulation of calcite (Saarinen, pers. comm.). In the sediments between 2741 and 2526 cm, $CaCO_3$ varies between 10 and 60 wt% around a mean value of c. 30 wt% (Fig. 3). The sub-section with Roman Pb (2726–2693 cm) shows a decline of $CaCO_3$ from 30 wt% to c. 10 wt% in its lower part and a $CaCO_3$ content of c. 10 wt% in its upper part (Fig. 5). By analogy with the lower varved section, a decrease in sediment accumulation is likely for the upper half of the Pb-contaminated sediment sequence. Between 2741 cm (0 AD/BC) and 2726 cm (beginning of Pb contamination) $CaCO_3$ decreases from 60 to 30 wt%. For a sediment-accumulation rate of 2.2 mm/a from 0 AD/BC until the beginning of the Pb pollution and a mean sedimentation rate of 1.8 mm/a for the Pb contaminated section, the onset of enhanced Pb influx would date to AD 68 and the influx of Roman Pb would have lasted 183 a. The An Loch Mór sedimentation record also documents for this assumption an enhanced influx of anthropogenic Pb over a relatively short period (starting in the 2nd half of the 1st century AD), especially if compared to the history of ancient Ag-production in the Mediterranean.

The derived $Pb_{anthr}[i]$ components of the individual TIMS-samples 22, 7, 23, and 24 plot in a narrow cluster within or close to the field defined by Pb ores from Rio Tinto (Fig. 6). The Pb_{anthr}-value of sample 6 shows a higher thorogenic composition that falls into the Pb isotopic variation range of Pb ores from Linares. The Pb pollutions of all balanced TIMS-samples, however, could as well originate from Pb emissions at British mining sites (Fig. 6). The anthropogenic Pb component of sample 6, alternatively, may be seen as a mixture of Pb from Rio Tinto and Carthagena or any other Spanish mining site with Pb isotope compositions similar to that of Carthagena, without any significant contribution of British Pb. The typical Pb isotope composition of carbonate-hosted Pb ores in the Irish Midlands (Dixon et al., 1990) and in SW Ireland (Rohl and Nedham, 1998; Fig. 6) is less radiogenic than the balanced anthropogenic Roman Pb component in the An Loch Mór sediments. Significant contributions from these sources therefore are unlikely. Rohl and Nedham (1998) and Northover et al. (2001)

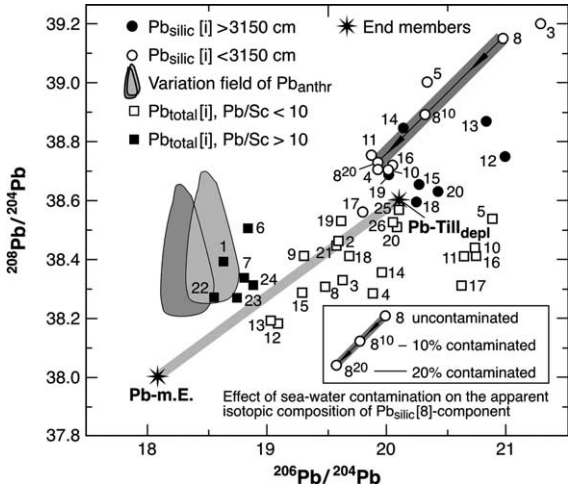

Fig. 7. $^{206}Pb/^{204}Pb$–$^{208}Pb/^{204}Pb$ diagram showing the measured Pb-isotopic composition of the sediment samples (Table 3), the end members Pb-m.E. and Pb-Till$_{depl}$ used for Pb-modelling and the calculated isotopic composition of the siliciclastic Pb components (Pb$_{silic}[i]$) of sediment samples with Pb/Sc < 10 (Table 5). The balanced Pb$_{silic}[i]$ components of most of the early Holocene sediments (samples 15, 18, 19, and 20) fall in a narrow field close to Till$_{depl}$, whereas the individual Pb$_{silic}[i]$ components of sediments deposited after c. 5500 cal. BP are characterised by distinctly higher thorogenic composition. This implies influx of remote dust with higher $^{208}Pb/^{204}Pb$. The estimates for the Pb-isotopic composition of the siliciclastic Pb component of these samples would be shifted to lower $^{208}Pb/^{204}Pb$ values, if the isotopic composition of seawater was influenced by Pb released from the dust input (cf. modelling of sample 8). The fields for anthropogenic Pb are for reference only.

studied the Pb isotope composition of Cu and bronze tools from Ireland (see also discussion in O'Brien, 2004). Lead of these artefacts reflects the Pb isotope composition of polymetallic mineral deposits mined in Ireland during the Bonze Age. Lead of these artefacts is typically less radiogenic than the anthropogenic Roman Pb in the An Loch Mór sediments (Fig. 6). A possible reactivation of the related Bronze Age mining sites for the exploitation of galena and extraction of Ag during the time of the Roman Empire is not supported by the results. Galena in/or above Ordivician rocks of SE-Ireland (Fig. 6) is characterised by a more radiogenic Pb isotopic compositions and in principle could represent a source for Roman Pb in the An Loch Mór sediments. Ireland, however, has never been occupied by the Romans and there exists no substantial archaeological evidence for ancient mining of galena and cuppelation of Ag by its Celtic inhabitants during the time of the Roman Empire.

The nearest major Roman mining districts are those of Asturia (Oviedo), Sierra Morena (Rio Tinto), and Carthagena on the Iberian Peninsula, Mendips, Cornwall, N. Devon and Shropshire in Britain, and minor deposits in the former Roman province of Gaul (for ancient mining of Pb ores, see Wright, 1888; Patterson, 1971, 1972; Nriagu, 1993, 1996; Shepherd, 1993; Weisgerber, 1993; Johnson, 1980; Cary and Scullard, 1992; and Fig. 1). The prevailing westerly wind directions do not favour wind transport of Pb-contaminated dust-particles from these mining districts to western Ireland at present. Depending on the weather situation, however, episodic transport of Pb emissions from these sites is possible.

The elevated influx of anthropogenic Pb could originate from Pb emissions at mining sites in Britain. The final Roman invasion of Britain occurred in AD 43 during the rule of Claudius. During a period of less than 40 a, essentially all mineral areas had been conquered (Wright, 1888). Roman pigs and ingots of Pb that were lost during their transport from British mining sites largely date between AD 49 and AD 169 (Johnson, 1980), which suggests that mining of British argentiferous galena peaked during that period. The Pb-isotopic composition of the Roman-Pb in the An Loch Mór sediments, however, provides no evidence that it originates from British sources only. Mining and processing of Pb ores on the Iberian Peninsula also may contribute to the Pb-pollution. The total production of Ag on the Iberian Peninsula, however, had reached its zenith in the 1st century BC and is assumed to have declined once the exploitation of near-surface British ores had started (Shepherd, 1993; Nriagu, 1993; Patterson, 1972). Silver production during the time of the Roman Empire had already declined in the 3rd century AD when the exploitation of Pb ores became increasingly limited by the engineering capabilities of the Romans (Patterson, 1972).

The decline of the Western Roman Empire around AD 400 was accompanied by a general decline of Pb-mining in western Europe until the early Medieval period. To the authors' knowledge, substantial Pb mining during Late Antiquity in the western Mediterranean is known only from the Iberian Peninsula during the economically prosperous reign of the Visogods (Martínez-Cortizas et al., 1997 and references therein). Enhanced Pb/Sc at 2650 cm (c. AD 500) may document Pb emissions from metallurgical processing of Pb ores in Iberia by the Visogods.

The Pb/Sc-profile also shows minor maxima in older sediment sections below 2710 cm (before AD 0). The Pb/Sc increase at 2770 cm (c. 100 BC) falls

in the period of the Roman republic. Requirements for Ag by the gradual increase of Ag-coinage in the Roman economy from the 3rd century BC, forced the exploration and mining of argentiferous Pb ores (Cary and Scullard, 1992). At this time, the Romans had no access either to the Pb ore deposits of the western Mediterranean in Gaul, and on the Iberian Peninsula, or to the major Pb ore deposits of Britain, Belgium, and Germany. In the course of the Punic wars, the Romans gained control over the important argentiferous Pb ore deposits on the Iberian Peninsula. The Roman conquest of the Iberian Peninsula, which lasted nearly the whole of the 2nd century BC, first allowed extensive exploitation of these ores on a large scale. Even earlier, the Carthaginians had succeeded in ejecting the Greeks from the greater parts of the Spanish coasts (Cary and Scullard, 1992). The minor Pb/Sc peak at 2780 cm (c. 210 BC) might be associated with an expansion in the mining and processing of argentiferous Pb ores on the Iberian Peninsula by the Carthaginians under Hannibal (cf. Shepherd, 1993 and references therein).

5.5. Comparison with other European records of atmospheric Roman Pb pollution

5.5.1. Onset and duration

The An Loch Mór sedimentation record clearly documents distinctly enhanced influx of anthropogenic Pb over a period of less than 200 a during the 1st and 2nd century AD. There are implications for minor Pb contamination by ancient mining activities during several sedimentation intervals before and after this period. A compilation of data on influx of Roman Pb from various palaeoenvironmental records is given in Table 6. There is a documented Pb increase for the Engbertsdijksveen peat deposit (Netherlands) between c. 750 BC and AD 300 (40 samples; van Geel et al., 1989; for updated chronostratigraphy see: Kilian et al., 2000) and Featherbed Moss (Derbyshire, UK) between 700 BC and AD 500 (Lee and Tallis, 1973). The Dutch as well the British bog records are from sites with significant land use during the late Bronze and Iron Ages. Human disturbance of the vegetation cover will have increased the airborne input of local and regional soil particles, which has not been considered for these two data sets. Thus, the general increase of Pb concentrations over periods of 600 and 1200 a, respectively, could largely reflect increased soil erosion.

More reliable estimates for the dating of maximum Pb-deposition and the duration of increased anthropogenic Pb-influx are available from 3 Swedish peat and lake records (Tab. 6; Brännvall et al., 1997). Although probable variations in the influx of siliciclastic matter have not been considered, Pb-isotopic data (ICP-MS) provide additional evidence for influx of excess anthropogenic-Pb. Only a very limited number of Pb-contaminated 1-cm samples demonstrate the influx of Roman-Pb in the peat records. The Store Moss record ($n = 4$) may document the most reliable estimate for the time of the maximum influx of Roman Pb (~AD 80). The given ages for the maximum influx of Roman Pb are AD 120 for Lake Rudegyl and 170 BC for Lake Gårdsjön (Table 6). New investigations on 11 Swedish lake records demonstrate significantly enhanced influx of Pb in Sweden over a period of less than 300 a with a maximum after 0 AD/BC (Renberg et al., 2001).

The Roman Pb-anomaly in the sediments of Lake Schalkenmehrener Maar and Lake Meerfelder Maar in the NW Eifel, Germany, cover less than 230 a (Schettler and Romer, 1998). A short duration of Pb pollution (AD 85–AD 199) is also documented from Lake Belau of northern Germany (Garbe-Schönberg et al., 1998). In a study of a Swiss bog-record, variable influx of siliciclastic matter has been considered by normalisation using Sc (Shotyk et al., 1998). Distinct enhanced influx of excess Pb is detected for a relative short period after 150–116 BC (age range gives the dating uncertainty). In a peat record from the Northwestern Iberian Peninsula (Penido Vello bog), the detection and quantification of anthropogenic Pb has been analytically performed by extraction of Al and Pb using 1 N KCl (Martínez-Cortizas et al., 1997). Excess-Pb is calculated by geochemical mass balance using the Pb/Al background of leachates from uncontaminated samples. Such an approach sensitively detects surface-bound exchangeable Pb, which may be represented to a significant portion by the dissolved influx of geogenic Pb. Anthropogenic Pb in fine glass-spherules and in post-depositional pyrite are not detected by such an analytical approach that may underestimate the content of anthropogenic Pb. Since there was no corresponding increase of Zn in the leachates, enhanced geogenic dissolved-influx of trace-elements in the contaminated section of the peat bog is unlikely. Therefore, the continuously sampled Pb-record from the Penido Velo bog reliably documents enhanced influx of Pb for northwestern Spain between 300 BC and AD 250. New studies on two peat bogs in northwestern Spain (referred to in Renberg et al., 2001) date the onset of distinctly enhanced Pb-influx

Table 6
Compilation of Roman lead anomalies in peat, bog, and lake deposits

Location		Sampling resolution	Number of contaminated samples	Anomaly identification	Timing of increased Pb deposition	Pb-flux (mg/m^{2}a)
Peat and bog deposits						
1[a]	Etang de la Gruere, Jura mountains (CH)		10	Pb/Sc	Distinct increase of Pb/Sc after 2066–2100 cal. BP (150–116 BC)	Max 0.4
2[b]	Engbertsdijksveen (NL)	1 cm (each 10 cm)	40	Pb_{total}	~750 BC–AD 300	<3.8
3[c]	Featherbed Moss (Derbyshire,GB)	1 cm (each 5 cm)	9	Pb_{total}	General increase ~700 BC–AD 500	~1.6
4[d]	Penido Vello bog (SP)	5 cm (continuously)	10	KCl-leachable Pb	~300 BC–AD 250 (uncalibrated)	~0.5
5[e]	Önneby Mosse (S)	1 cm (each 10 cm)	1	Pb_{total}	Before AD 120	
6[e]	Trolls Mosse (S)	1 cm (each 10 cm)	1	Pb_{total}	After 280 BC	
7[e]	Store Mosse (S)	1 cm (each 10 cm)	4	Pb_{total}	Max.~AD 80	~0.4
8[f]	Tor Royal (Devon, GB)	1 cm (each 25 cm)	1	Pb_{total}	after 160–390 BC before AD 660–450	
Lakes						
9[g]	Gardsjön (S)	1 cm (each 10 cm)	1	Pb_{total}	Max.~170 BC	
10[g]	Rudegyl (S)	1 cm (each 10 cm)	3	Pb_{total}	Max. ~AD 120	
11[h]	Belau, Schleswig-Holstein (GER)	~4 cm (each 16 cm)	4	Pb/Zr (Pb/Th)	AD 85–AD 261/(176 years)	3.0 (4.0)
12[i]	Meerfelder Maar (MFM), W.Eifel (GER)	1 cm (continuously)	11	Pb/Al	Floating varve chronostr. (~230 years)	2.7
13[i]	Schalkenmehrener Maar, W.Eifel (GER)	1 cm (continuously)	12	Pb/Al		3.8

[a] Given maximum Pb flux from original work Shotyk et al. (1998). Estimation of peat accumulation is based on ^{14}C dates of peat samples measured by decay counting (3000 BP, 2110 BP, and 1350 BP), the given calibrated age was calculated using CALIB REV, version 3.0.3.

[b] Cal.^{14}C dates were recalculated by wiggle matching (Kilian et al., 2000). Pb flux estimated here as mean over ~200 a using porosity 0.85, $\rho = 1.4$ g/cm^3, and a Pb excess of 10 ppm. Variable influx of siliciclastic matter was not considered. Source: van Geel et al. (1989).

[c] Site near Derbyshire lead mining area. Pb flux estimated here as mean over ~400 a using porosity 0.85, $\rho = 1.4$ g/cm^3, and a Pb excess of 15 ppm. Source: Lee and Tallis (1973), dating based on comparison with ^{14}C dated pollen records from the region.

[d] Pb flux estimated here as mean over ~400 a (40 cm) using porosity 0.85, $\rho = 1.4$ g/cm^3, and a Pb excess of 2.5 ppm. Source: Martínez-Cortizas et al. (1997), uncalibrated ^{14}C dates.

[e] Pb flux estimated here for Store Mosse as mean over ~250 a using porosity 0.85, $\rho = 1.4$ g/cm^3, and a Pb excess of 2 ppm. Source: Brännvall et al. (1997), AMS ^{14}C dates of bulk samples from peat calibrated using Radiocarbon Calibration Program 3.0 (Stuiver and Reimer, 1993).

[f] Source: West et al. (1997), Radiocarbon dates calibrated after Stuiver and Reimer (1993).

[g] Source: Brännvall et al. (1997), AMS ^{14}C dates of terrestrial macrofossils calibrated using Radiocarbon Calibration Program 3.0 (Stuiver and Reimer, 1993).

[h] Pb flux re-calculated here using a porosity of 0.75 and $\rho = 2.5$ g/cm^3. Values in brackets based on Pb/Th normalization. Source: Garbe-Schönberg et al. (1998). Age model based on varve counting and calibrated ^{14}C dates.

[i] Pb flux calculated for a porosity of 0.85 and $\rho = 1.6$ g/cm^3. Source: Schettler and Romer (1998). Duration of enhanced Pb flux in Schalkenmehrener Maar adapted from correlation with varved sediments of the Meerfelder Maar.

slightly before 0 BC/AD and show a maximum for the influx of anthropogenic Pb during the 1st or 2nd century AD, when Pb-mining on the Iberian Peninsula already might have declined.

5.5.2. Flux rates

Flux rates for anthropogenic Roman Pb derived for various European lake and bog records that were recovered near and far from former Roman mining sites (Fig. 1, Table 6) vary within one order of magnitude (0.3–3.8 mg $m^{-2}a^{-1}$). Considering that Pb-flux estimates for Engelbertsdijksveen, Featherbed Moss and Tor Royal (see Table 6) could represent overestimates, as increased detrital-bound geogenic Pb input originating from intensified land use has not been accounted for, the variation of flux rates may become even smaller. The enhanced flux rates for Lake Schalkenmehrener Maar and Lake Meerfelder Maar might reflect their proximity to Roman mining sites. Flux rates of anthropogenic Pb for 1.95 mm annual sediment accumulation, 1.8 g cm^{-3} density of the solid sediment, and a porosity of 0.5 were calculated. Background values of Pb/Sc = 4.2 [ppm/ppm] and Pb/Y = 0.71 yield between 2693 and 2726 cm mean annual deposition-rates for anthropogenic Roman Pb of 24.4 or 23.5 mg m^{-2} a^{-1}, respectively. On average, the influx of anthropogenic Pb exceeds the one of geogenic Pb by a factor of 1.6. The derived flux rates show a high variability (0–68 mg m^{-2} a^{-1}, Pb/Sc-budget). The unexpectedly high flux rates for Roman Pb in the An Loch Mór sediments distinctly exceed that of other European records (Table 6). This may reflect that An Loch Mór sediments monitor aeolian Pb deposition above an area larger than the surface of the lake. There may be substantial contributions via input of sea spray aerosols and from the catchment of the lake. This seems likely, since the retention of Pb in the karstic catchment of An Loch Mór should be rather low due to the absence of any significant clay mineral content in the sparse soil cover of the karst. Considering additionally the possible focusing of the particle flux in the lake basin, the real mean atmospheric deposition of Roman Pb on Inis Oírr may have been in the same order of magnitude as for records from central Europe (c. 1 mg m^{-2} a^{-1}).

6. Synopsis

An Loch Mór is located far from any Roman mining site. The sedimentation record of An Loch Mór, therefore, documents ancient atmospheric Pb-pollution on a large geographic scale. The short duration found for the distinctly elevated influx of anthropogenic Pb contrasts with the longer historic record on the development and extent of ancient mining of argentiferous galena and its metallurgical processing. Such a short period of ancient Roman Pb pollution is also obtained from high-resolution German lake records (Lake Belau, Schleswig Holstein (Garbe-Schönberg et al., 1998), Maar Lakes of the western Eifel (Schettler and Romer, 1998), and varved lake records from northern Sweden, Lake Koltjärn 62°57′N 20°59′W and Lake Grånästjärn 64°53′N 20°38′W, which document significant Pb pollution between c. 0 and 300 AD (Brännvall et al., 2001)). The Maar Lakes from the western Eifel are located to the SE and near an important Roman Pb-mining district (Mechernich, Aachen). Since the Pb-isotopic composition of the anthropogenic Pb in the Eifel-records is similar to the one of mined regional Pb ores, the short duration (~230 a) of the enhanced influx of anthropogenic Pb was interpreted in the context of the mining of regional argentiferous Pb ores (Schettler and Romer, 1998). The varved sediments of Lake Belau document a distinctly enhanced influx of Roman Pb (~2 mg m^{-2} a^{-1}, Table 6) over a period of 114 a (AD 85–AD 199), which due to the prevailing westerlies was interpreted to originate from Pb emissions in Britain. Roman Pb contamination in the lake records from Germany (Schettler and Romer, 1998; Garbe-Schönberg et al., 1998), Sweden (Renberg et al., 2001; Brännvall et al., 2001), and western Ireland (this study) show a similar duration and a similar order of magnitude.

The high portion of Pb_{anthr} in Pb_{total} in the An Loch Mór sediments between 2693 and 2726 cm allows a reliable characterisation of the Pb isotopic signatures of the Roman Pb contamination. The Pb-isotopic signature of the anomalous An Loch Mór sediments indicates possible contributions from Spanish and/or British Pb ore deposits. Transport from these Pb sources to Ireland is not favoured by the dominant westerly winds. Occasional meteorological conditions, however, give southern (55 days a^{-1}) and eastern (46 days a^{-1}) winds in west- ern Ireland (meteorological data from 1881–1990; Gerstengarbe and Werner, 1993). Southern winds are commonly accompanied by rain, whereas easterly winds, which tend to be connected with anti-cyclonic systems centred over north Britain and Fennoscandinavia, are normally associated with dry conditions; precipitation is only to be expected for rare North Atlantic Fennoscandian and Fennoscandian high pressure situations (10 days a^{-1}). Wet deposition of

airborne anthropogenic Pb should be more efficient than dry-deposition of Pb-contaminated aerosols, which is best illustrated by the spatial distribution of radioactive fallout after the Chernobyl reactor accident (Eliassen, 1990). From these considerations, contributions of Pb released at Spanish mining sites appear as likely as or even more likely than Pb-contributions from the more closely located mining sites in Britain, Belgium, or Germany (Fig. 1).

Although there has been significant extraction of Ag from argentiferous Pb ores on the Iberian Peninsula since the Phoenician period, distinctly enhanced atmospheric influx of Roman Pb into An Loch Mór occurred only for a limited period during the time of the Roman Empire. The decline of aeolian deposition of Roman anthropogenic Pb dates long before the decline of the Western Roman Empire. It certainly reflects the exhaustion of known surface-near galena-deposits by the Romans. Recently investigated palaeoenvironmental archives document ancient pollution by anthropogenic Pb with higher reliability. Lead contamination falling in the time of the Roman Empire is distinctly more prominent than that related to earlier periods. This might document that early Ag-extraction was carried out on a small scale. The introduction and use of larger cupellation furnaces might have resulted in a higher ascent of Pb emissions within the troposphere, which is a primary requirement for long-range distribution of large amounts of Pb aerosols from former smelting sites. Since improved metallurgical technologies are likely to have been adopted more or less coevally at all major Roman mining sites, the higher anthropogenic Pb-concentrations of individual European palaeoenvironmental records would reflect a technological advance made during the time of the Roman Empire. Thus, enhanced aeolian influx of Roman Pb may have proceeded across Europe more synchronous than previously assumed and may generally represent a mixture of Pb emissions from several remote sources. The distinct variability in the influx of Roman Pb for the An Loch Mór sedimentation record certainly does not document changes in the Roman mining and smelting activities, instead it reflects changes in the palaeo-climatic regime that favoured or limited the wind-transport of Pb emissions from ancient smelting sites to western Ireland.

Acknowledgement

Dr. H. Usinger and his co-workers (University of Kiel, Germany) are thanked for the recovery of three sediment profiles in An Loch Mór by a modified piston-core technique provided by the University of Kiel. We acknowledge technical support by Andreas Hendrich, Ursula Kegel and Cathrin Schulz (all GFZ-Potsdam). We thank Dr. P. Dulski and his laboratory team at the GFZ-Potsdam for ICP-MS measurements of Pb and Dr. F. Dermott (Dublin) for constructive comments. The authors wish to acknowledge financial support received from the European Union (4th Framework Programme (phase 2), Climate and Environment, Contract No. ENV4-CT97-0557) and the GFZ-Potsdam. We thank Dr. Henry Lamb and an anonymous reviewer for their valuable comments to an earlier draft of the manuscript.

Appendix. Abbreviation list

EVPT	evapotranspiration in the hydrological catchment of the lake
Hydrogenic	geochemical characteristics of solid materials originating from solid/water interaction in the exosphere. As particularly used in this manuscript: element specific enrichment of trace elements or change of REE-signatures in sediments by dissolved influx (see Schettler et al., in press for Ce_N/Ce_N^*-minima in sedimentation periods with enhanced seawater influx)
LIAL	late iron age lull
MOR1,2,3	defines sediment cores from An Loch Mór
$Ia(b) - x \ldots Va(b) - x$	defines the number of the 2 m drives for the coring site, (a) upper (b) lower 1 m section
YD	Younger Dryas, Late glacial period with climatic deterioration
L_m	mean local carboniferous limestone
T_m	mean till, modelled as fine fraction of regional drift (silt:clay = 1:1)

(*continued on next page*)

Appendix (*continued*)

$Till_{clay}$	clay fraction of regional drift
$Till_{silt}$	silt fraction of regional drift
$^{silic}Till_{silt}$	non-calcareous fraction of $Till_{clay}$
$^{silic}Till_{silt}$	non-calcareous fraction of $Till_{silt}$
Pb-X	end members considered for Pb isotope mass balances
Pb-$Till_{depl}$	Pb isotope composition of clastic YD sediments
Pb-m.E.	estimated seawater Pb isotope composition (m.E. = marine end member)
Pb-L_m	Pb isotope composition of L_m
Pb_{total}	total Pb concentration
^{exc}Pb(total)	Pb-excess calculated by mass balance, based on Pb/Al_2O_3 of YD sediments
^{exc}Pb(r)	Pb-excess relative to Pb(total) in %
$^{exc}Pb,Sc,Y(n)$	calculated excess of Pb, Sc or Y, respectively based on Pb(Sc,Y)/Al_2O_3 of YD sediments, normalised per 1 wt% Al_2O_3
^{exc}Pb(anthr)	general Pb-excess originating from Pb emissions at ancient mining sites
$^{exc}Pb^{Sc}$(anthr)	Pb-excess calculated by mass balance, based on a Pb/Sc-background value given in Section 5.2
$^{exc}Pb^{Y}$(anthr)	Pb-excess calculated by mass balance, based on a Pb/Y-background value given in Section 5.2
^{exc}Pb(geog)	Pb-excess calculated by: ^{exc}Pb(total) minus $^{exc}Pb^{Sc}$(anthr)
$Pb_{anthr}[i]$	anthropogenic Pb component of individual sediment samples
$Pb_{exc}[i]$	Pb-excess of individual sediment samples
$Pb_{silic}[i]$	portion of hypothetical geogenic Pb which originates from siliciclastic influx with Pb/Al_2O_3 (ppm/wt%) = 2.5
$Pb_{total}[i]$	total Pb concentration of sample (i).

References

Andrew, C.J., Crowe, R.W.A., Finlay, S., Pennell, W.M., Pyne, J.F. (Eds.), 1986. The Geology and Genesis of Mineral Deposits in Ireland. Irish Association for Economic Geology, Dublin.

Arribas Jr., A., Tosdal, R.M., Wooden, J.L., 1991. Lead isotope constraints on the origin of base- and precious-metal deposits from southeastern Spain. In: Pagel, M., Leroy, J.L. (Eds.), Source, Transport and Deposition of Metals. Balkema, Rotterdam, pp. 241–244.

Brännvall, M.-L., Bindler, R., Emteryd, O., Nilsson, M., Renberg, I., 1997. Stable isotope concentration records of atmospheric lead pollution in peat and lake sediments in Sweden. Water Air Soil Poll. 100, 243–252.

Brännvall, M.-L., Bindler, R., Emteryd, O., Renberg, I., 2001. Four thousands years of atmospheric lead pollution in northern Europe: a summary from Swedish lake sediments. J. Paleolim. 25, 421–435.

Candelone, J.-P., Hong, S., 1995. Post-Industrial Revolution changes in large-scale atmospheric pollution of the northern hemisphere by heavy metals as documented in central Greenland snow and ice. J. Geophys. Res. 100 (D8), 16.605–16.616.

Cary, M., Scullard, H.H., 1992. A History of Rome: Down to the Reign of Constantine. MacMillan, Houndmills.

Chambers, F.M., Daniell, J.R.G., Hunt, J.B., Molloy, K., O'Connell, M., 2004. Tephrostratigraphy of An Loch Mór, Inis Oírr, W. Ireland: significance for Holocene tephrochronology on the north-east Atlantic seaboard. Holocene 14, 703–720.

DeMenocal, P., Ortiz, J., Guilderson, T., Sarntheim, M., 2000. Coherent high- and low-latitude climate variability during the holocene warm period. Science 288, 2198–2202.

Dixon, P.R., LeHuray, A.P., Rye, D.M., 1990. Basement geology and tectonic evolution of Ireland as deduced from Pb isotopes. J. Geol. Soc. London 147, 121–132.

Dulski, P., 2001. Reference materials for geochemical studies: New analytical data by ICP-MS and critical discussion of reference values. Geostand. Newslett. 25, 87–125.

Eliassen, A., 1990. Chernobyl: a summary case study with emphasis on the transport and deposition to Scandinavia. In: Knap, A.H. (Ed.), The Long-range Atmospheric Transport of Natural and Contaminant Substances. Proc. NATO Adv. Res. Inst.. Kluwer Acad. Publ., Dordrecht, pp. 149–162.

Garbe-Schönberg, C.-D., Wiethold, J., Butenhoff, D., Utech, Chr., Stoffers, P., 1998. Geochemical and palynological record in annually laminated sediments from Lake Belau (Schleswig Holstein) reflecting paleoecology and human impact over 9000a. Meyniana 50, 47–70.

Gerstengarbe, F.-W., Werner, P.C., 1993. Katalog der Großwetterlagen Europas nach P. Hess and H. Brezowsky 1881–1992. Berichte des Deutschen Wetterdienstes, Offenbach (a.M.) 113.

Graney, J.R., Halliday, A.N., Keeler, G.J., Nriagu, J.O., Robbins, J.A., Norton, S.A., 1995. Isotopic record of lead pollution in lake sediments from the northeastern Unites States. Geochim. Cosmochim. Acta 59, 1715–1728.

Haggerty, R., Budd, P., Rohl, B., Gale, N.H., 1996. Pb-isotopic evidence for the role of Mesozoic basins in the genesis of Mississippi Valley-type mineralization in Somerset, UK. J. Geol. Soc. London 153, 673–676.

Hong, S., Candelone, J.-P., Patterson, C.C., Boutron, C.F., 1994. Greenland Ice Evidence of Hemispheric Lead Pollution Two Millennia ago by Greek and Roman Civilizations. Science 265, 1841–1843.

Jennings, S.G., O'Dowd, C.D., O'Connor, T.C., McGovern, F.M., 1991. Physical characteristics of the ambient aerosols at Mace Head. Atmos. Environ. 25A, 557–562.

Johnson, S., 1980. Later Roman Britain. Routledge and Kegan Paul, London.

Johnston, J.D., 1999. Regional fluid flow and the genesis of Irish Carboniferous base metal deposits. Mineral Dep. 34, 571–598.

Kempter, H., Görres, M., Frenzel, B., 1997. Ti and Pb concentrations in rainwater-fed bogs in Europe as indicators of past anthropogenic activities. Water Air Soil Poll. 100, 367–377.

Kilian, M.R., van Geel, B., van der Plicht, J., 2000. 14C AMS wiggle matching of raised bog deposits and models of peat accumulation. Quatern. Sci. Rev. 19, 1011–1033.

Lee, J.A., Tallis, J.H., 1973. Regional and historical aspects of lead pollution in Britain. Nature 245, 216–218.

LeHuray, A.P., Caulfield, J.B.D., Rye, D.M., Dixon, P.R., 1987. Basement controls on sediment-hosted Zn–Pb deposits: a Pb isotope study of carboniferous mineralization in central Ireland. Econ. Geol. 82, 1695–1709.

Livett, E.A., Lee, J.A., Tallis, J.H., 1979. Lead, zinc and copper analyses of British blanket peats. J. Ecol. 67, 865–891.

Martínez-Cortizas, A., Pontevedra-Pombal, X., Nóvoa Muñoz, J.C., García-Rodeja, E., 1997. Four thousand years of atmospheric Pb, Cd and Zn deposition recorded by the ombrotrophic peat bog of Penido Vello (Northwestern Spain). Water Air Soil Poll. 100, 387–403.

McGovern, F.M., Krasenbrink, A., Jennings, S.G., Georgi, B., Spain, T.G., Below, M., O'Connor, T.C., 1994. Mass measurements of aerosols at Mace Head, on the west coast of Ireland. Atmos. Environ. 28, 1311–1318.

Molloy, K., O'Connell, M., 2004. Holocene vegetation and land-use dynamics in the karstic environment of Inis Oírr, Aran Islands, western Ireland: pollen analytical evidence evaluated in light of the archaeological record. Quatern. Int. 113, 41–64.

Northover, J.P., O'Brien, W., Stos, S., 2001. Lead isotopes and metal circulation in beaker/early bronze age Ireland. J. Irish Archaeol. 10, 25–48.

Nriagu, J.O., 1993. Lead and Lead Poisoning in Antiquity. Wiley, New York.

Nriagu, J.O., 1996. A History of global metal pollution. Science 272, 223–224.

Nriagu, J.O., Pacyna, J.M., 1988. Quantitative assessment of worldwide contamination of air, water and soils by trace metals. Nature 333, 134–139.

O'Brien, W., 2004. Ross Island. Mining, metal and society in early Ireland. Bronze Age Studies 6, Department of Archaeology, National University Galway.

O'Connell, M., 1994. Main area: Ireland [site data]. In: Frenzel, B., Gläser, B. (Eds.), Palaeoclimate Research, Evaluation of Land Surfaces Cleared from Forests in the Roman Iron Age and the Time of the Migrating Germanic Tribes Based on Regional Pollen Diagrams, Vol. 12. Gustav Fischer, Stuttgart, pp. 50–54.

O'Connell, M., Mitchell, F.J.G., Readman, P.W., Doherty, T.J., Murray, D.A., 1987. Palaeoecological investigations towards the reconstruction of the post-glacial environment at Lough Doo, County Mayo, Ireland. J. Quatern. Sci. 2, 149–164.

Patterson, C.C., 1971. Native copper, silver and gold accessible to early metallurgists. Am. Antiq. 36, 286–321.

Patterson, C.C., 1972. Silver stocks and losses in ancient and Medieval times. The Economic History Review 25 (Second Series), 205–235.

Renberg, I., Bindler, R., Brännvall, M.-L., 2001. Using the historical atmospheric lead-deposition record as a chronological marker in sediment deposits in Europe. The Holocene 11, 511–516.

Renberg, I., Person, M.W., Emteryd, O., 1994. Pre-industrial atmospheric lead contamination detected in Swedish lake sediments. Nature 368, 323–326.

Rohl, B.M., 1996. Lead isotope data from the Isotrace Laboratory, Oxford: Archaeometry Data Base 2, Galena from Britain and Ireland. Archaeometry 38, 165–180.

Rohl, B.M., Nedham, S., 1998. The circulation of metal in the British Bronze Age: the application of lead isotope analysis. British Museum Occasional Paper 102. London.

Romer, R.L., Förster, H.-J., Breitkreuz, C.h.r., 2001. Intracontinental extensional magmatism with a subduction fingerprint: the late Carboniferous Halle Volcanic Complex (Germany). Contrib. Mineral. Petrol. 141, 201–221.

Rosman, K.J.R., Chisholm, W., Hong, S., Candelone, J.-P., Boutron, C.F., 1997. Lead from Carthaginian and Roman Spanish mines isotopically identified in Greenland Ice dated from 600 B.C. to 300 A.D. Environ. Sci. Technol. 31, 3413–3416.

Schell, W.R., Tobin, M.J., Novak, M.J.V., Wieder, R.K., Mitchell, P.I., 1997. Deposition history of trace metals and fallout radionunclides in wetland ecosystems using ^{210}Pb chronology. Water Air Soil Poll. 100, 233–239.

Schettler, G., Romer, R., 1998. Anthropogenic influences on Pb/Al and lead isotope signature in annually layered Holocene Maar lake sediments. Appl. Geochem. 13, 787–797.

Schettler, G., Romer, R.L., O'Connell, M., Molloy, K., submitted. Holocene climatic variation and post-glacial sea-level rise geochemically recorded in the sediments of the brackish karst lake An Loch Mór, western Ireland. Boreas.

Shepherd, R., 1993. Ancient Mining. Elsevier Applied Science, London.

Shotyk, W., Weiss, D., Appleby, P.G., Cheburkin, A.K., Frei, R., Gloor, M., Kramers, J.D., Reese, S., van der Kaap, W.O., 1998. History of atmospheric deposition since 12,370 ^{14}C yr BP from peat bog, Jura Mountains, Switzerland. Science 281, 1635–1640.

Stos-Gale, Z., Gale, N.H., Houghton, J., Speakman, R., 1995. Lead isotope data from the Isotrace Laboratory Oxford: Archaeometry Data Base 1, Ores from the Western Mediterranean. Archaeometry 37, 407–415.

Stuiver, M., Reimer, P.J., 1993. High-precision decadal calibration of the radiocarbon time scale, AD 1950- 6000BC. Radiocarbon 35, 215–230.

Stuiver, M., Reimer, P.J., Bard, E., Beck, J.W., Burr, G.S., Hughen, K.A., Kromer, B., McCormac, F.G., van der Plicht, J., Spurk, M., 1998. INTCAL98 Radiocarbon Age Calibration, 24,000-0 cal BP. Radiocarbon 40, 1041–1083.

Taylor, S.R., 1964. Abundance of chemical elements in the continental crust: a new table. Geochim. Cosmochim. Acta 28, 1273–1285.

Telmer, K., Bonham-Carter, G.F., Liza, D.A., Hall, E.M., 2004. The atmospheric transport and deposition of smelter emissions: evidence from the multi-element geochemistry of snow, Quebec, Canada. Geochim. Cosmochim. Acta 68, 2961–2980.

TIMECHS, 2001. TIMECHS: Timing and Mechanisms of Holocene Climate Change in NW Europe. Final Report to EU Commission, Brussels, Contract No. ENV4-CT97-0557, NUI Galway.

Tullet, M.T, 1980. A dust-fall of Saharan origin on 15 May 1979. J. Earth Sci. Roy. Dublin Soc. 3, 35–39.

Tullet, M.T., 1984. Saharan dust-fall in Northern Ireland. Weather 39, 151–152.

van Geel, B., Bregman, R., van der Molen, P.C., Dupont, L.M., van Driel-Murray, C., 1989. Holocene raised bog deposits in the Netherlands as geochemical archives of prehistoric aerosols. Acta Bot. Neerl. 38, 467–476.

Weisgerber, G., 1993. Römischer Erzbergbau in Deutschland. Archäologie in Deutschland, Sonderheft, pp. 55–62.

West, S., Charman, D.J., Grattan, J.P., Cherbukin, A.K., 1997. Heavy metals in Holocene peats from South West England: Detecting mining impacts and atmospheric pollution. Water Air Soil Poll. 100, 343–353.

Wright, T., 1888. Roman mining operations in Shropshire and North Wales. Trans. Shropshire Archaeolog. Soc. 11, 272–290.